Naval Research Laboratory

Washington, DC 20375-5320

NRL/MR/7600--15-9637

Volume 1.
NRL SSD Research Achievements: 1960–1970

Jill Dahlburg
George Doschek
Christoph Englert
Russell Howard
W. Neil Johnson
Michael Kowalski
Dennis Socker
Kent Wood

Space Science Division

October 30, 2015

REPORT DOCUMENTATION PAGE

Form Approved
OMB No. 0704-0188

1. REPORT DATE *(DD-MM-YYYY)*	2. REPORT TYPE	3. DATES COVERED *(From - To)*
30-10-2015	Memorandum Report	1960 – 1970

4. TITLE AND SUBTITLE

Volume 1. NRL SSD Research Achievements: 1960–1970

5a. CONTRACT NUMBER

5b. GRANT NUMBER

5c. PROGRAM ELEMENT NUMBER

6. AUTHOR(S)

Jill Dahlburg, George Doschek, Christoph Englert, Russell Howard,
W. Neil Johnson, Michael Kowalski, Dennis Socker, and Kent Wood

5d. PROJECT NUMBER

5e. TASK NUMBER

5f. WORK UNIT NUMBER

7. PERFORMING ORGANIZATION NAME(S) AND ADDRESS(ES)

Naval Research Laboratory
4555 Overlook Avenue, SW
Washington, DC 20375-5320

8. PERFORMING ORGANIZATION REPORT NUMBER

NRL/MR/7600--15-9637

9. SPONSORING / MONITORING AGENCY NAME(S) AND ADDRESS(ES)

Naval Research Laboratory
4555 Overlook Avenue, SW
Washington, DC 20375-5320

10. SPONSOR / MONITOR'S ACRONYM(S)

NRL

11. SPONSOR / MONITOR'S REPORT NUMBER(S)

12. DISTRIBUTION / AVAILABILITY STATEMENT

Approved for public release; distribution is unlimited.

13. SUPPLEMENTARY NOTES

14. ABSTRACT

The 1960s produced a cornucopia of seminal space science discoveries, with Naval Research Laboratory (NRL) Space Science Division (SSD) instrumentation flown on rockets, on the National Aeronautics and Space Administration (NASA) Orbiting Geophysical Observatories (OGOs) and Orbiting Solar Observatories (OSOs), and via the Department of Defense (DoD) Space Test Program (STP). This summary provides a technical overview of some of the major NRL SSD research achievements during this decade, 1960–1970.

15. SUBJECT TERMS

Space Science History

16. SECURITY CLASSIFICATION OF:			17. LIMITATION OF ABSTRACT	18. NUMBER OF PAGES	19a. NAME OF RESPONSIBLE PERSON
					Jill Dahlburg
a. REPORT	b. ABSTRACT	c. THIS PAGE			19b. TELEPHONE NUMBER *(include area code)*
Unclassified Unlimited	Unclassified Unlimited	Unclassified Unlimited	Unclassified Unlimited	46	(202) 767-6343

Standard Form 298 (Rev. 8-98)
Prescribed by ANSI Std. Z39.18

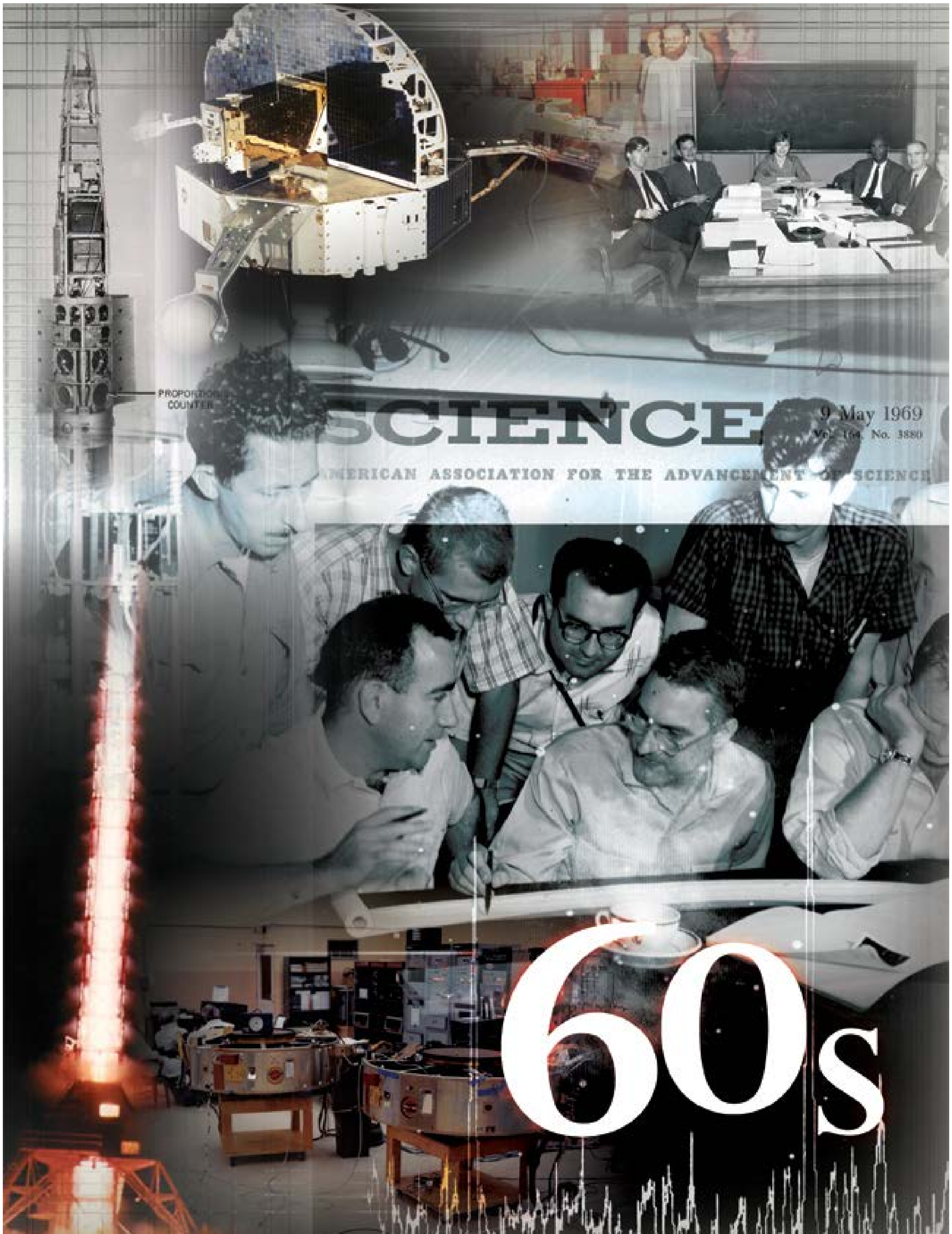
PROPORTIONAL
COUNTER
SCIENCE
9 May 1969
AMERICAN ASSOCIATION FOR THE ADVANCEMENT OF SCIENCE
60s

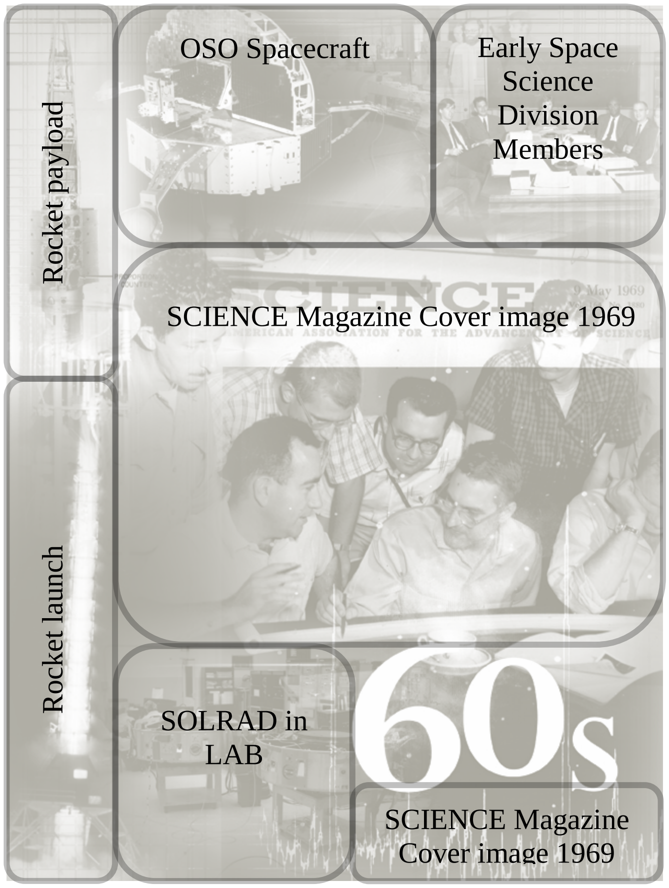

The 1960s produced a cornucopia of seminal space science discoveries, with NRL Space Science Division instrumentation flown on rockets, on the NASA Orbiting Geophysical Observatories (OGOs) and Orbiting Solar Observatories (OSOs), and via the DoD Space Test Program (STP). In astrophysics research, experiments on rocket flights led to the discovery of many new cosmic X-ray sources; the first detection of X-rays from the Crab Nebula and an estimate of the volume of the emission, from a tour-de-force lunar occultation rocket experiment; and the First Detection of X-Ray Pulsations from the Crab Pulsar that matched the radio and optical pulsations. In upper atmospheric physics, experiments on the OGOs resulted in: the first measurements proving that interstellar hydrogen (H) flows into the solar system and mapping the H distribution to 10 solar radii; the first global mapping of oxygen and nitrogen airglow; the discovery of ultraviolet (UV) tropical arcs; the discovery of Lyman-α rocket plumes in the thermosphere; the first mapping of auroral UV emissions; and early mapping of the H distribution in the exosphere. From the STP P72-1 spacecraft, NRL/SSD scientists obtained the first mapping of interstellar helium (He) within the solar system; the first remote sensing of global He in the thermosphere and the first mapping of ionized helium (HE II) in the plasmasphere; and the discovery of energetic He atom precipitation from the ring current via EUV remote sensing. Solar physics experiments on rockets and the OSOs resulted in: the first X-ray image of the Sun; high-resolution spectroscopy of the solar spectrum from about 1 to 25 Å including line identifications and the beginning of the development of plasma diagnostics for highly ionized atoms; the first image of the solar corona taken outside of a total solar eclipse (rocket flight); and the investigation of the hard X-ray spectrum of solar flares. The first of a series of 11 solar radiation satellites (SOLRADs) carrying SSD X-ray and longer wavelength sensors was launched in June 1960 by the Naval Center for Space Technology, verifying the direct relationship between solar X-ray variability and the strength of the Earths ionosphere. Subsequent SOLRAD satellites collected valuable X-ray and ultraviolet monitoring data throughout the 1960s until 1973.

PREFACE

We offer these summaries of Naval Research Laboratory (NRL) Space Science Division (SSD) research achievements to provide a technical overview of NRL space science accomplishments from the beginning of the Division in 1952 through the first decade of the 21^{st} century.

These summaries are presented in five Volumes:

Volume 1. NRL SSD Research Achievements: 1960-1970
Volume 2. NRL SSD Research Achievements: 1970-1980
Volume 3. NRL SSD Research Achievements: 1980-1990
Volume 4. NRL SSD Research Achievements: 1990-2000
Volume 5. NRL SSD Research Achievements: 2000-2010

The importance of space science basic research in support of naval needs was robustly championed by Homer Newell, the Division's second Superintendent, who noted to the US Congress in 1957, "A strong basic research program is essential to continuing vitality of applied R&D in missiles or any other military or peacetime applications. New facts, new ideas, new techniques, new materials, new instruments, all come from the basic research effort..." As the dozens of summaries in these five Volumes tremendously attest, extraordinary ranges of research and results have been achieved.

To document significant SSD historical accomplishments, Drs. George Doschek and Jill Dahlburg requested current and former SSD researchers to contribute technical achievement summaries to these Volumes on the basis of their personal memories about the scientific activities in which they were involved. The contributions received were then loosely organized by decade into these five featured Volumes, after being edited for clarity by George Doschek, Tanisha Lucas, and Jill Dahlburg.

George Doschek would like to express his gratitude to all the researchers who have contributed to these summaries, and particularly to those with whom he has personally worked. The SSD has and is currently continuing to provide substantive and significant contributions to the developments of experimental space science since its origins after World War II, and it has been a privilege to be part of this effort. These Volumes convey stories about curiosity, hopes, and aspirations of scientists fascinated by exploration of the Universe with instrumentation placed beyond the Earth's atmosphere.

Tanisha Lucas wishes to acknowledge that she has benefited from the advice, assistance, and all of the contributions that our researchers put into these documents. She wishes to express her gratitude to the NRL SSD researchers for their remarkable scientific contributions, her appreciation for the advice on content and organization for this book provided by Dr. Jill Dahlburg, and her many thanks to Dr. George Doschek for closely working with her in compiling and arranging these Volumes.

Jill Dahlburg acknowledges with pleasure and gratitude the request from Dr. John Montgomery, NRL Director of Research, that these Volumes be developed. They present a unique account of exceptional contributions from the NRL SSD broad-spectrum research, development and experimentation program to study the atmospheres of the Sun and the Earth, the physics and properties of high-energy space environments, and solar activity and its effects on the Earth's atmosphere, and to transition these capabilities to operational use.

Finally, George, Tanisha and Jill would together like to thank Ms. Kathryn Grouss who worked with us to prepare these Volumes during 2014, for her exceptional cooperation, professionalism, assistance and advice, and to Dr. Angelina Callahan, NRL Associate Historian, for her many beneficial insights and suggestions, and her unswerving encouragement.

George Doschek, *NRL SSD Historian*
Tanisha Lucas, *NRL SSD Research Achievements Managing Editor*
Jill Dahlburg, *NRL SSD Superintendent*

Manuscript approved December 15, 2014.

Table of Contents

Overview of the NRL Space Science Division 1960's Decade

At the US Naval Research Laboratory (NRL), the story of space research formally began in 1952, with the creation of the NRL Atmospheres and Astrophysics (A&A) Division under the direction of Dr. John Hagen, and a Division charter to perform research and development in the field of space science. The Division's second Superintendent, Homer Newell (1956-1958), continued A&A's seminal space research both at NRL and then later at NASA (see, for instance, NASA SP-4211: "Beyond the Atmosphere, Early Years of Space Science," by Homer Newell). During Dr. Newell's NRL tenure from 1944-1958 he assembled a world-leading space science team, which outstandingly included Herbert Friedman and Richard Tousey, to carry out scientific research from rockets, and he was also a key visionary and architect of the National Aeronautics and Space Administration (NASA) Orbiting Geophysical Observatories (OGO) and the Orbiting Solar Observatories (OSO) programs to which NRL contributed fundamentally. Following Dr. Newell's departure to the newly formed NASA in 1958, Herbert Friedman assumed leadership of NRL space science as the third A&A Division Superintendent (1958-1982). Dr. Friedman oversaw the renaming of the Division from A&A to Space Science, in 1968, and in 1982 he transitioned the Division to the leadership of Dr. Herbert Gursky, who served as SSD's fourth Superintendent from 1982-2006. Jill Dahlburg, the fifth and current SSD Superintendent, was appointed to the position in 2007 following her service as Acting SSD Superintendent from May 2006. The scope of the NRL Space Science Division encompasses theoretical, experimental and numerical research of geophysics science and technology, solar and heliospheric physics, and the high-energy space environment, and the conception, design, fabrication, integration, test, operation and experimentation with forefront space instrumentation, for the purpose of enabling Navy/ Marine Corps and wider DoD robust access to space assets.

The 1960's produced a cornucopia of seminal space science discoveries, with NRL Space Science Division instrumentation flown on rockets, on the NASA OGO and OSO satellites, and via the Department of Defense (DoD) Space Test Program (STP).

In the area of geophysics science and technology, NRL SSD 1960's experiments on the OGOs resulted in: the first measurement proving that interstellar hydrogen (H) flows into the solar system and mapping the H distribution to 10 solar radii; the first global mapping of oxygen and nitrogen airglow; the discovery of ultraviolet (UV) tropical arcs; the discovery of Lyman-α rocket plumes in the thermosphere; the first mapping of auroral UV emissions; and early mapping of the H distribution in the exosphere. From the STP P72-1 spacecraft NRL SSD scientists obtained the first mapping of interstellar helium (He) within the solar system; the first remote sensing of global He in the thermosphere and the first mapping of ionized helium (He II) in the plasmasphere; and, the discovery of energetic He atom precipitation from the ring current via EUV (extreme ultraviolet) remote sensing. This Volume's Essay 60's.1 provides an overview of this seminal research.

NRL SSD 1960's solar and heliospheric physics experiments on rockets and on the OSOs resulted in: the first X-ray image of the Sun; high resolution spectroscopy of the solar spectrum from about 1 - 25 Å and 170 – 4000 Å including line identifications and the beginning of the development of plasma diagnostics for highly ionized atoms; the first image of the solar corona taken outside of a total solar eclipse (rocket flight); and, the investigation of the hard X-ray spectrum of solar flares. Essay 60's.2 describes this exciting science.

High energy space environment research was fundamentally advanced in the 1960's, by means of the first of a series of eleven solar radiation satellites (SOLRADs) carrying SSD X-ray and longer wavelength sensors, which was launched in June 1960 by the NRL organization that is now known as the Naval Center for Space Technology. These space experiments verified the direct relationship between solar X-ray variability and the strength of the Earth's ionosphere. Subsequent SOLRAD satellites with SSD instrumentation on board collected valuable X-ray and ultraviolet monitoring data, throughout the 1960's until 1973. In Essay 60's.3, core highlights of this work are provided. Further, SSD instrumentation flown on rockets led to the discovery of many new cosmic X-ray sources in the 1960's; the first detection of X-rays from the Crab Nebula and an estimate of the volume of the emission from a tour-de-force lunar occultation rocket experiment; and, the first detection of X-ray pulsations from the Crab Pulsar that matched the radio and optical pulsations. This work is overviewed in Essay 60's.4, and also is comprehensively described in "The Astronomer's Universe," by Herbert Friedman.

60's.1: Contributions in Upper Atmospheric and Magnetospeheric Physics, Comets, Interplanetary Gas, and Radiation Transport Theory: 1960's and 1970's

Contributed by Robert R. Meier *(retired from NRL)*

1.0 1960's

This decade was an era of discovery for upper atmospheric research. Virtually every mission flown made major discoveries. Following in the footsteps of E. O. Hulburt, an early researcher of the upper atmosphere, NRL quickly became a world leader in observing and understanding the state and behavior of the upper atmosphere and ionosphere. Major new space-based tools were developed for imaging and spectroscopic remote sensing of the near space environment that ultimately would lead to operational missions such as Special Sensor Ultraviolet Limb Imager (SSULI) on the *Defense Meteorological Satellite Program* (*DMSP*) spacecraft.

2.0 OGO-3

Discovery of atomic hydrogen in the interplanetary medium

In the 1960's and even earlier, the Sun was believed to be a classical Strömgren star whose ionizing radiation and particle fluxes would have prevented interstellar neutral atoms from penetrating the solar system. But the work by Phillip Mange and Robert Meier at NRL demonstrated that the hydrogen UV glow beyond 10 Earth radii, measured by the NRL far ultraviolet (FUV) radiometer on the *Orbiting Geophysical Observatory 3* (*OGO*) satellite (launched in June 1966 into a highly elliptical orbit), varied in concert with solar activity. They were able to establish that hydrogen atoms were indeed close enough to the Sun to scatter the solar Lyman alpha flux and mimic its variability. This work initiated an entirely new paradigm of the interaction of the solar system with the local interstellar medium (ISM), namely that neutral atoms can actually pass into the inner heliosphere, thereby invalidating the early Strömgren theory that was thought to be the governing concept.

Mapping of the outermost hydrogen geocorona to 10 Earth radii

Reliable altitude profiles of atomic hydrogen were measured at geocentric distances between 5 and 16 Earth radii, again from OGO-3. The hydrogen content could be explained with a model of the exosphere (the region of atmosphere above about 500 km where collisions are rare) in which atoms at high altitudes were on bound ballistic trajectories, or on hyperbolic escaping trajectories, or in orbit around the Earth. Strong variations in H density occurred over periods of order weeks. This mission set the baseline for the understanding of planetary coronae.

3.0 OGO-4

OGO-4 was launched into low Earth orbit in July 1967 and operated successfully until January 1969. The NRL far ultraviolet radiometer program, led by Phillip Mange, set the stage for FUV remote sensing of the upper atmosphere as a discipline. A large number of discoveries resulted from this mission. Some are enumerated below.

Solving the hydrogen geocorona problem

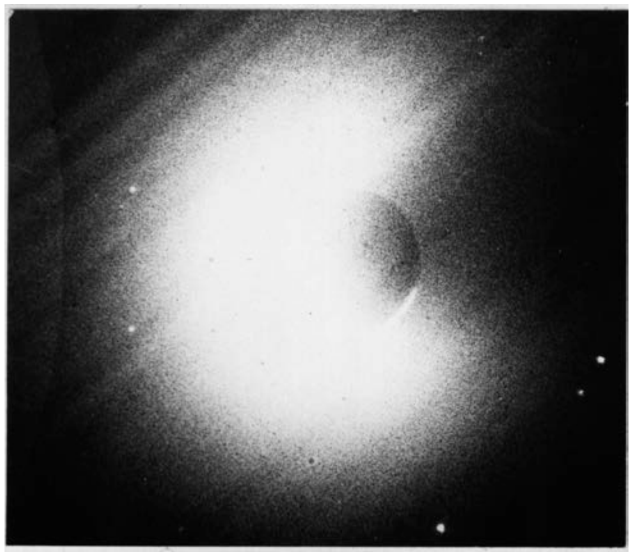

Fig. 60s.1.1 – Image of the hydrogen geocorona at Lyman-α (121.6 nm) taken from the lunar surface during the Apollo-16 mission (credit: NRL).

Although nearly two decades had passed since the Division's third Superintendent, H. Friedman, and colleagues discovered the hydrogen Lyman alpha glow (at 121.6 nm), the origin of the nighttime emission had not been identified. Early radiation transport modeling found that scattering of solar Lyman alpha photons into the Earth shadow could not account for the relatively bright signal observed. The detailed measurements from *OGO-4* showed a continuous and decreasing emission from day to night. This glowing hydrogen cloud was finally explained when R. Meier developed a new radiation scattering model that extended to more than 10 Earth radii altitude. Hydrogen at such high altitude can much more easily scatter solar Lyman alpha radiation into the Earth's shadow and produce the nightglow, thereby explaining the observations. This picture of the Earth being enveloped in a huge hydrogen cloud was confirmed by *OGO-3*, *OGO-4*, *OSO-4* (*Orbiting Solar Observatory-4*) and various rocket measurements of Lyman alpha carried out by P. Mange. Later G. Carruthers' electrographic camera was flown to the Moon during the Apollo-16 mission, where it became the first observatory on the moon. Stunning full-earth images were obtained, including one at Lyman alpha that showed the Earth enveloped in a huge cloud of hydrogen. One of the Lyman alpha images from the Apollo-16 camera is shown above in Fig. 60s.1.1. Modeling of such images by the Space Science Division team demonstrated consistency with the data. As well, a large hydrogen "tail" was found to extend well into the anti-solar direction.

First global mapping of atomic oxygen and molecular nitrogen in the thermosphere

Two of the *OGO-4* radiometers were dedicated to observing O and N_2 FUV emissions. R. Meier and D. Prinz (NRL) undertook comprehensive studies of the emissions and demonstrated that they are produced mainly by photoelectron impact excitation. They demonstrated that variability in the emissions is related to changes in the thermosphere on various time and geographic scales. This understanding led to the proposal by NRL scientists that the emissions could be used to satisfy Department of Defense (DoD) requirements for monitoring neutral densities in the thermosphere. Later this proposal was validated by analyses of the NASA/*TIMED* (*Thermosphere*, *Ionosphere*, *Mesosphere Energetics and Dynamics*) satellite FUV measurements by the GUVI (Global Ultraviolet Imager) experiment beginning in 2002 (by R. Meier and colleagues) and later by the space flight of the NRL RAIDS (Remote Atmospheric and Ionospheric Detection System) and the SSULI operational system. SSULI continues to fly as an operational sensor on DMSP satellites.

Discovery of the oxygen UV tropical arcs in the ionosphere

Atomic oxygen FUV emissions at 130.4 and 135.6 nm emanating from the tropical ionospheric region were noticed in the nightglow by NRL's Grady Hicks. Along with Talbot Chubb, Hicks showed that the emissions tracked the geomagnetic dip equator, but were located symmetrically on either side by 12-15 degrees, and by inference were related to tropical ionospheric processes. Radiative recombination of ionospheric oxygen ions was ultimately found to be the principal production mechanism, along with a small contribution from $O^+ + O^-$ mutual neutralization. This discovery led to the realization that the ionosphere could be sensed remotely in the FUV spectral region. The SSULI developed at NRL was based on this concept (as well as remotely sensing the neutral thermosphere in the FUV). A global image of the arcs produced by Carruthers' camera on the lunar surface can be seen below.

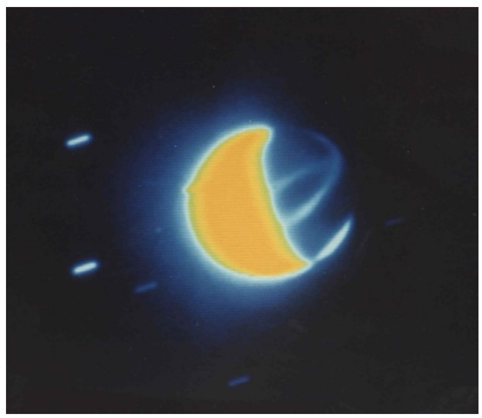

Fig. 60s.1.2 – Image of the dayglow and tropical ionospheric arcs in the light of oxygen at 135.6 nm. Taken from the lunar surface during the Apollo-16 mission. Auroras are present near the north and south poles. The arcs are seen extending into night, to the right of the terminator in the center of the Earth image. (Carruthers camera image, credit: NRL)

Discovery of hydrogen Lyman alpha plumes in the upper atmosphere following missile launches

While analyzing *OGO-4* satellite data, Grady Hicks discovered hydrogen Lyman alpha emission following the passage of missiles through the upper atmosphere. The detections were clustered around various launch sites, including the Eastern and Western Test Ranges and the USSR launch site. Work by Hicks, Chubb and Meier demonstrated the deposition of hydrogenous exhaust products above 100 km results in a local enhancement of hydrogen, which resonantly scatters Lyman alpha radiation from the Sun and from the geocorona, and produces a far ultraviolet contrail. The discovery was documented in Hicks, Chubb, & Meier (1976), NRL Report 8061. More recent observations from the GUVI experiment on the NASA/*TIMED* mission resulted in actual images showing enormous contrails as large as 15,000 km between extreme edges. An example is seen in Fig. 60s.1.3 on the next page. The plume was observed on March 4, 2002, about 80 hours following the launch of the Space Shuttle, Space Transport System STS-109.

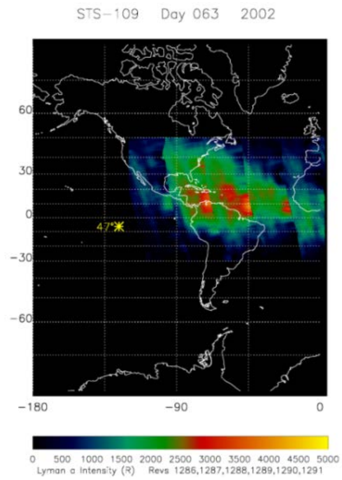

Fig. 60s.1.3 – Image of the STS-109 Space Shuttle hydrogen plume at Lyman-α (121.6 nm) (credit: NRL).

FUV auroras

Although rocket experiments had demonstrated that FUV emissions are present in the auroral zone, the OGO-4 mission provided the first comprehensive synoptic measurements. Talbot Chubb and Grady Hicks published a seminal paper showing how the hydrogen, oxygen and nitrogen emissions mimicked the auroral oval and how the emissions distinguish between proton and electron auroras.

Discovering the nature of the ionosphere

As early as 1956, NRL flew mass spectrometers on rockets to measure the composition of the ionosphere. In the 1960's and 1970's, the NRL Ionosphere Section, including Charles Johnson, James Young and Julian Holmes, made a number of major discoveries, including the overall composition of ionospheric regions, the domination of the E-region by NO^+, the metallic ion composition of sporadic E layers, and the radiation sources that maintained the E-region at night. This latter work resulted in the discovery of H Lyman beta, He 58.4 nm and He^+ 30.4 nm emissions from the geocorona, the interplanetary medium, and the plasmasphere, respectively.

Discovery of atomic oxygen 63μm radiative cooling in the upper atmosphere

A rocket experiment launched by Paul Feldman and Douglas McNutt, both of NRL, discovered infrared emission of atomic oxygen at 63 microns and published their findings in 1969. Radiative cooling at 63 microns is the principal energy loss process in the middle and upper thermosphere.

4.0 1970's

This decade continued the exploration by SSD scientists of the terrestrial environment and interplanetary space with new technology that included FUV imaging and extreme ultraviolet (EUV from 10 to 100 nm) detection systems. The consequence was a host of major new discoveries about the Earth's environment, as well as such extraterrestrial processes as the flow of interstellar gas into the solar system and the behavior of comets. This decade of research provided direct pathways to remote sensing of the upper atmosphere and ionosphere that led in turn to the space flight of operational systems.

Apollo-16 discoveries (see essay 70s.1)

Detection of interstellar helium flowing into the solar system

The 1972 launch of the NRL EUV experiment on the DoD Space Test Program *STP 72-1* satellite opened up that spectral regime for exploration in the same way that the NRL *OGO-4* experiment initiated comprehensive study of the FUV. The He 58.4 nm emission observed locally by the NRL rocket experiment in 1969 could now be studied on a global scale. After a year of observing, NRL's Charles Weller and Robert Meier were able to map the glowing helium in the night sky and found that it had a broad diffuse character, except for a bright region around 90 deg right ascension and 0 deg declination (see map below). They were able to show that interstellar helium flowing into the solar system is gravitationally focused by the Sun into a "wake" of much denser helium than is present in the upstream direction. From the *STP 72-1* data, they were able for the first time to derive the helium density, the flow speed and direction, and the temperature of the incoming gas (from the extent of spreading in the downstream direction).

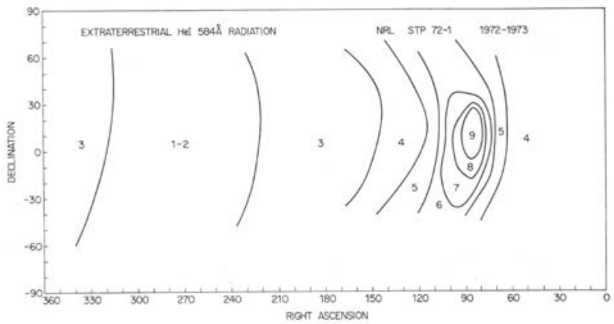

Fig. 60s.1.4 – Contour map of the interstellar atomic helium emission at 58.4 nm produced by backscattering of sunlight as the atoms are gravitationally focused around the Sun (credit: NRL).

Inner magnetospheric imaging

Charles Johnson and colleagues proposed that the He^+ 30.4 nm emission observed at night in their 1969 rocket observations originated in the plasmasphere (the ionized region between the ionosphere and the magnetosphere) and, consequently, would lead to a new innovative way to image the inner magnetosphere. A few years later, Meier and Weller demonstrated that the predictions of a new plasmasphere scattering model quantitatively matched the He^+ 30.4 nm emission. The *STP 72-1* mission returned global-scale photometric data that demonstrated conclusively the feasibility of studying the plasmasphere optically. The schematic Fig. 60s.1.5 is a three-dimensional rendering of an idealized plasmasphere along with its observation from the *STP 72*-1 satellite at 750 km. The conic section is the instrument field of view, looking outward through the Earth's shadow into the sunlit plasmasphere.

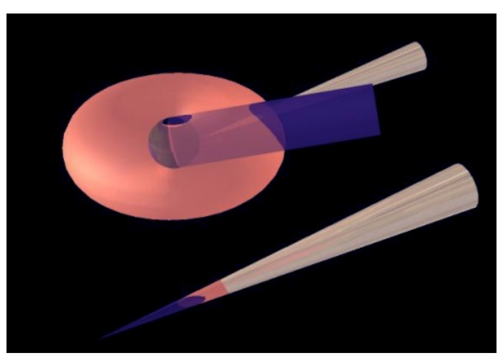

Fig. 60s.1.5 – 3D rendering of an idealized plasmasphere on 15 November 1972 simulating the STP 72-1 viewing geometry. The Sun shines from the lower left. The STP 72-1 instrument field-of-view is represented by the yellow cone. Note the complex geometric intersection of the plasmasphere with the Earth's shadow. An expanded view of the interaction of the instrument field-of-view and shadow is also shown (see Meier et al. 1998, JGR, 103, 17505; credit: NRL).

Fig. 60s.1.6 shows an equatorial view of *STP 72*-1 He II 30.4 nm column emission rates. Arrows indicate the anti solar direction; the shadow is shown by the shaded region. The field of view (FOV) of the EUV experiment is shown in the upper left panel. Column emission rates are plotted radially outward from the satellite position. The data show that the plasma structure of the magnetosphere can change significantly for different observing conditions. Subsequently, Meier and colleagues showed that the *STP 72*-1 data could be inverted to return geophysical plasmspheric parameters, such as the boundaries and the variation of plasma density with altitude. These investigations proved beyond a doubt that inner magnetospheric imaging is feasible. With the launch of an EUV imager on the NASA IMAGE satellite in 2000, the concept discovered at NRL had evolved into a powerful tool for studying the interaction of the solar wind and the terrestrial plasma system on a global scale.

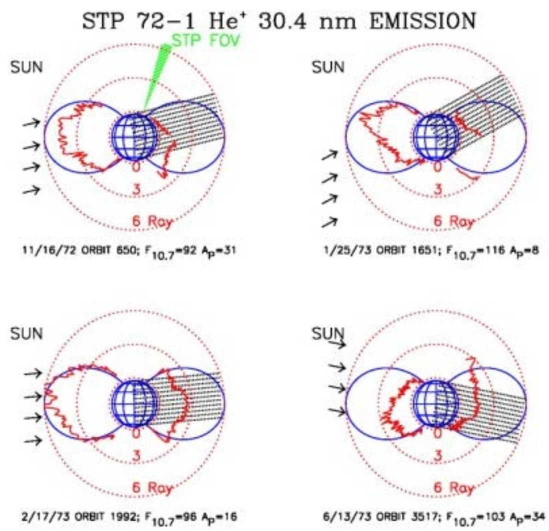

Fig.60s.1.6 – Equatorial display of STP 72-1 He II 30.4 nm column emission rates. Geomagnetic latitude and longitude are drawn on the Earth at the center. L = 4 dipole lines are shown. Arrows indicate the anti-solar direction; the shadow is shown by the shaded region. The field-of-view of the EUV instrument is shown in the upper left panel. The innermost dotted circle indicates the satellite altitude. Column emission rates are plotted radially outward from the satellite position. The zero emission rate level coincides with the orbital location, and the 3 and 6 R levels are also shown as dotted circles (credit: NRL).

First optical mapping of helium atoms in the thermosphere

The *STP 72-1* mission also measured helium 58.4 nm radiation in the thermosphere during the day. This dayglow is sensitive to the abundance of helium. Donald Anderson, Meier and Weller showed that the helium concentration can be retrieved with appropriate radiative transport modeling. The observations demonstrated that such phenomena as the winter helium bulge, with densities one to two orders of magnitude larger than the summer concentrations, could easily be detected with remote sensors.

Discovery of energetic helium atoms precipitating from the ring current

STP 72-1 observed an unexpected emission at 30.4 nm that was centered on the magnetic equator. The emission intensity and spatial structure varied with geomagnetic activity. Meier and Weller found that the emission came from very energetic helium (energy from 10 to greater than 100 keV) atoms that originated as ions in the plasmasphere that had been neutralized by charge exchange with hydrogen atoms. The atoms precipitate into the thermosphere where they are re-ionized into excited states of He^+, followed by radiation at 30.4 nm.

First FUV spectrographic images of comets

NRL's George Carruthers and Chet Opal obtained the first FUV spectrographic images of a comet from an NRL sounding rocket launched on January 8, 1974. Dramatic images of a huge hydrogen cloud around Comet Kohoutek produced a wealth of information about the gases being released as this "Christmas" comet passed through the inner solar system. The huge cloud of hydrogen surrounding Comet Kohoutek is shown in the upper left panel of the figure; a visible image (to scale) is shown below for comparison. Isophotes of the Lyman alpha image are shown to the right along with a model that was fit to the observations by R. Meier, H. Uwe Keller (Max Planck Institut für Aeronomie), Opal and Carruthers. Their analysis yielded much new information about the comet properties, including water and hydrogen production rates, velocity distributions and inferred photochemical processes, as well as the survival time against charge exchange loss to the solar wind. A similar version of the Carruthers camera was flown on Skylab-4, and obtained additional images of Comet Kohoutek during the period November 26, 1973 through January 10, 1974. These observations traced the variation of the cometary coma as it passed through perihelion. The NRL comet team also launched other sounding rocket missions that obtained spectacular images of Comet West in 1976 and Comet Halley in 1986.

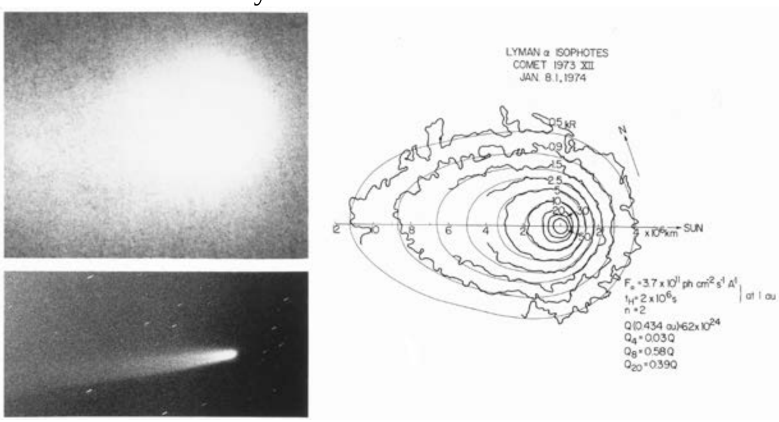

Fig.60s.1.7 – Upper left panel: hydrogen Lyman-α image of Comet Kohoutek. Lower left: coincident visible light image on the same scale, illustrating the huge size of the hydrogen coma. Right panel: contours of Lyman-α brightness along with a model (smooth lines). Physical parameters of the model are indicated (Meier et al. 1976, Astron. & Astrophys., 52, 283. Credit: NRL).

First complete solution of the resonance radiation transport problem in optically thick media

The transport of resonance radiation in very thick media is exceedingly complex due to the angular dependence of the photon frequency shift during the scattering process. In 1978, R. Meier and NRL's Jong-Sen Lee developed an innovative Monte Carlo model that not only included all features of the multiple scattering process, but also could be adapted to the solution of physically realistic problems in planetary atmospheres. For the first time, they were able to accurately model the atomic oxygen 130.4 nm emission lines that are prominent in the spectra of the atmospheres of Earth, Mars and Venus, and extract the relative oxygen concentrations.

5.0 Summary

The 1960s and 1970s constituted the second generational epoch of the space age, following the earlier explorations of space by Friedman, Tousey, Chubb, and colleagues. These were decades of exciting discoveries in many fields as new probes were sent into space on all manner of vehicles, ranging from sounding rockets and balloons to the astronaut-carrying Apollo spacecraft that reached the lunar surface. This brief history can only scratch the surface of the major advances pioneered in the Space Science Division at NRL and barely convey the excitement and enthusiasm of the scientists, engineers and technicians, as well as the support staff, who made it all possible.

60's.2: The Orbiting Solar Observatories (OSOs)

Contributed by George A. Doschek and Russell A. Howard

1.0 The *OSO* Program and Spacecraft

The *OSO* program was conceived of by Dr. John Lindsay, head of the Solar Physics Branch at Goddard Space Flight Center and formerly from NRL. Lindsay had served in the NRL Optics Division in 1957 and 1958. He had done some work at NRL with Herbert Friedman**,** the Division's third Superintendent**,** on solar X-ray space experiments before the *OSO* program was conceived. The solar instruments on the *OSOs* were designed to investigate the UV (Ultraviolet), EUV, X-ray, and gamma ray emission from the Sun, and later, the white light corona. This was the first major NASA orbiting satellite program to investigate the physics of the solar atmosphere and was spectacularly successful. Nine spacecraft were successfully launched. Prior to launch they were designated as *OSO-A* through *OSO-I* and after launch became *OSO-1* through *OSO-8* (one spacecraft was not successful). Ball Brothers Research Corporation (now Ball Aerospace) built the first seven *OSOs*; *OSO-8* was built by Hughes Aircraft. Two more *OSOs* were to be built, J and K, but instead were combined into one spacecraft that became the Solar Maximum Mission (SMM). General *OSO* information is given in the table below:

Table 60s.2.1

Spacecraft	Launch Date	NRL Involvement
OSO-1	07 March 1962	None
OSO-2	03 February 1965	X-ray Bursts (Chubb), White Light Corona (Tousey)
OSO-3	08 March 1967	None
OSO-4	15 October 1967	X-ray Detectors (Chubb), X-ray Spectrometers (Friedman), Geocoronal Lyman-α telescope (Kreplin)
OSO-5	22 January 1969	EUV Spectroheliograph (Purcell), X-ray Radiation Ion Chamber Photometer (Chubb)
OSO-6	09 August 1969	X-ray Spectroheliograph (Chubb, Kreplin)
OSO-7	29 September 1971	White Light Coronagraph and EUV Telescope (Tousey)
OSO-8	21 June 1975	EUV From Earth & Space (Weller)

The *OSO* spacecraft consisted of a spinning wheel that could spin up to 15 rpm to provide pointing stability. Above the wheel was a de-spun platform called the sail which carried instruments that could image the Sun. The sail was the prime real estate on the spacecraft and was also the home of the solar power cells. The wheel section contained instruments that could view the Sun while spinning, and the sail normally had two instruments that provided imaging. An interesting technological achievement was that power was generated in the sail section and the antenna was in the rotating section, so that power and signals had to be transmitted across the rotating joint – very few data errors were encountered in spite of this difficulty. An image of an *OSO* is shown in Figure 60s.2.1.

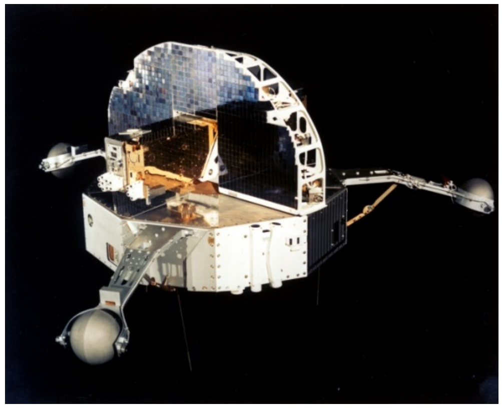

Figure 60s.2.1 – A typical NASA Orbiting Solar Observatory (OSO) spacecraft. The top part of the spacecraft is the sail and contains two instruments with 3-axis pointing stability. The wheel below spins and contains additional science instruments that can record data even though spinning (credit: NASA).

The most important instruments flown by NRL on the *OSOs* were sail-section X-ray spectrometer packages that flew on *OSO-4* and *OSO-6*, under the direction of Herbert Friedman, and a sail-section white light coronagraph on *OSO-7* under the direction of NRL's Richard Tousey. The X-ray instruments had considerable competition from X-ray spectrometers flown by Werner Neupert at Goddard Space Flight Center (GSFC) on *OSO-3* and *OSO-5*, as well as other spacecraft, and much was learned about the Sun's solar flare X-ray spectrum from all of these instruments. The coronagraph on *OSO-7* was without competition and it was with this instrument that SSD scientists discovered coronal mass ejections (CMEs). The discovery of CMEs is one of the foremost accomplishments of the Division's heliophysics program.

2.0 The SSD White Light Coronagraph on *OSO-7* and the Discovery of Coronal Mass Ejections

OSO-7 was launched from Cape Canaveral on 29 September 1971 by a Delta N rocket into a 33.1° inclination, low-Earth (initially 321 by 572 km) orbit, and re-entered the Earth's atmosphere on 9 July 1974. The second stage rocket did not work properly and put the spacecraft into an elliptic orbit with a spin, instead of a circular one. The spacecraft engineers were able to stop the spin, just before the battery power was depleted and the solar arrays could charge the battery. However, one of the two tape recorders failed at launch, further crippling the mission. While the basic design of all the *OSO* satellites was similar, the *OSO-7* was larger [total spacecraft mass was 635 kg (1397 lb)] than the *OSO-1* through *OSO-6*, with a larger squared-off solar array in the non-rotating sail, and a deeper rotating wheel section. The *OSO-7* spacecraft is shown in Figure 60s.2.2.

Figure 60s.2.2 – The OSO-7 spacecraft looked noticeably different than most of the other OSO spacecraft (credit: NASA).

The white light coronagraph on *OSO-7* was based on coronagraphs flown on rockets by NRL's Richard Tousey, Martin Koomen and colleagues. It featured a specially designed external occulter 76 cm from the instrument 26.4 mm diameter entrance aperture (see Figure 60s.2.3). The external occulter allowed the faint outer corona to be observed up to 10 solar radii from the solar disk. Coronagraphs without an external occulter could only observe out to about 2 solar radii at the time of *OSO-7*. In order to adequately suppress stray light, the instrument parameters were chosen such that the solar inner corona was occulted out to 3.0 solar radii, so the total field of view was an annular region surrounding the Sun from 3.0 solar radii out to 10 solar radii. In tests the coronagraph had a stray light level only 10^{-10} of the solar disk brightness. The brightness of the corona in the instrument field of view varied from 10^{-8} (3.0 solar radii) to 10^{-10} (10 solar radii) of the solar disk brightness.

Figure 60s.2.3 – The OSO-7 (NRL) white light coronagraph. The occulter boom blocks the light from the solar disk, which would overwhelm the light from the corona and coronal mass ejection by many orders of magnitude. The Sun is occulted naturally during a total solar eclipse when the moon becomes the occulter (credit: NRL).

The detector was a Westinghouse Secondary Emission Cathode (SEC) vidicon low light-level television camera tube. This tube had many good qualities for a coronagraph detector. These included ruggedness, compactness, low power consumption, high sensitivity and signal to noise ratio, storage, and long detector lifetime. A segmented polarizing filter was cemented to the vidicon fiber optics faceplate. Except for two narrow annular rings, the polarization is concentric and enhances the electron scattered corona. This emission is not enhanced in the annular rings. The vidicon contained a square detector area with what would now be called a 256 x 256 pixel array. Each pixel had a resolution at the Sun of 1.25 arc minutes. An *OSO-7* coronal image is shown in Figure 60s.2.4. The central white disk shows the size and location of the Sun.

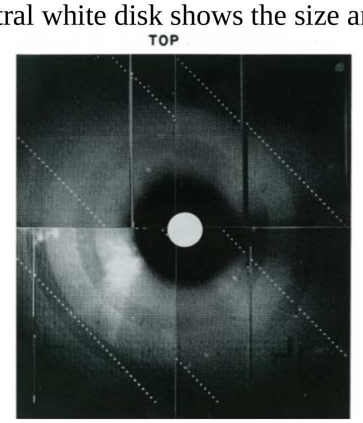

Figure 60s.2.4 – The total field-of-view of the NRL white light coronagraph. The coronal mass ejection (CME) can be seen in the lower left quadrant. The white light Sun is blocked by the occulter and the white disk has been inserted to show its location and size. The very dark area surrounding this disk is the area masked by the occulter. The corona is the extended emission in the images. The two darker annuli are due to polarizers put in the plane of the image. Million degree gas appears dark in the polarizer regions (credit: NRL/NASA).

The size of the NRL *OSO-7* coronagraph with external occulter stowed was 7.25 cm x 29 cm 120 cm and everything was installed in a box milled from a single block of magnesium alloy tooling plate. The complete instrument weighed 50 kg and dissipated 6.6 W when in operation. A short history and detailed description of the NRL instrument is given by Koomen, et al. (1975).

The *OSO-7* spacecraft and instruments were operated from Goddard Space Flight Center. The SSD team, consisting of physicist Charles Detwiler (NRL) and electronics technician David Roberts (NRL) made two trips a day to GSFC to command the coronagraph. The coronagraph could observe the full Sun within its field of view or a single quadrant of it. The data were stored on magnetic tape and processed in SSD by NRL's Dave Roberts, Jack Whitney and Russell Howard. Dave Roberts was one of the first people to see the coronagraph images. On 13 December 1971 what we now call a coronal mass ejection (CME) occurred. CMEs have two major components: a million degree coronal component that moves outwards in a shell-like shape that can look like a sphere but is most likely a magnetic flux rope with a shape more like a croissant. In addition to the million degree component, which has an amorphous, large-scale structure, there is a highly structured small-scale component which is the eruptive prominence that is part of the erupting magnetic structures. This component has a temperature more like 10,000 K. *OSO-7* saw part of the prominence structure as it passed through one of the corners of a coronagraph quadrant (see bottom left quadrant in Figure 60s.2.4). As told to the writer by Dave Roberts, when Guenter Brueckner, one of the Division scientists on the coronagraph team, saw a succession of images with the prominence material moving through the field of view (see Figure 60s.2.5, he immediately grasped the significance of the observation and got very excited. The coronagraph science team, including Richard Tousey, Martin Koomen, Guenter Brueckner, Russell Howard, and NRL's Donald Michels, realized that they had made a major discovery, and that solar outbursts such as they observed could have important adverse consequences on the near-Earth environment and electrical grids on the Earth itself. They measured the speed of the outburst material at about 600 miles/s and estimated sizes of about 20-40 times the Earth's size for the individual structures in the outburst.

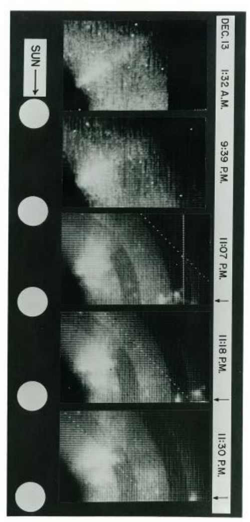

Figure 60s.2.5 – The NRL discovery images of the first observed coronal mass ejection (CME), December 13, 1971. The Sun is blocked by the occulter but indicated by the white disk on the left side of the figure. Note that the mass ejection (bottom right of image indicated by arrows), remains bright in the polarizer region. This is because the observed material has much lower temperatures than a million degrees and is part of the prominence ejecta that normally accompanies a CME. The coronal part of the CME was not observed (credit: NRL/NASA).

The scientists issued an NRL press release which was released on 10 January 1972 (appended). In this release they described possible consequences of solar eruptions on the Earth in terms of total energy involved and accelerated particles. More importantly, the SSD scientists realized the potential power of a solar coronagraph, stating in the press release: "The *OSO*-based coronagraph has given science an immensely improved capability to observe directly the size, density, speed and paths of these clouds, enabling project investigators to predict quite accurately the intensity, timing, and character of the effects to be expected on Earth whenever these emissions are on an earthbound course". A CME discovery paper was written by Richard Tousey (1973), then head of the SSD Rocket Spectroscopy Branch, the branch in which the coronagraph team resided. More CMEs were observed (e.g., Koomen, et al. 1974) and the coronagraph images were sent on a continuing basis to the NOAA for publication, and to Houston to prepare the astronauts for what they might see during the upcoming Skylab manned mission.

Prior to *OSO-7*, such dynamical phenomena in the outer corona had not been expected. Two coronagraphs had been launched on a rocket from White Sands, New Mexico on successive days and had shown that the solar corona changed on that time scale. The data rate for the coronagraph was 200 bps, requiring 45 minutes for a full image to be sent to the ground, perfectly adequate for the "stable" corona. The higher spatial and time resolution Skylab coronagraph observed many events, much more detailed and beautiful than those detected by the *OSO-7* coronagraph.

The discovery of CMEs has heralded a new era in space-based solar physics in both instrumentation and theory which continues to be one of the most important solar research areas. Furthermore, as the sophistication of space systems and our reliance on them increases, so, too, do our vulnerabilities to eruptive solar events such as flares and CMEs. Our increasing reliance on space-based systems involves both DoD and civilian areas (e.g., Global Positioning System) that are impacted by solar storms. The continuing research at NRL, both theoretical and experimental, to understand the origin of CMEs and flares and the mechanisms by which their effects propagate through the heliosphere and accelerate damaging high energy particles, will significantly improve our knowledge of the Sun-Earth connection.

3.0 The X-ray Spectrometers on *OSO-4* and *OSO-6* and the Investigation of the X-ray Spectrum of Solar Flares

The SSD X-ray spectrometer package shared the pointed section of the spacecraft with rastering EUV spectrometers flown by Harvard College Observatory, now part of the Center for Astrophysics. The crystal spectrometers consisted of flat crystals that scanned different wavelengths by rotating the crystals and detector units in steps of 0.1 degree. The crystals used were LiF (2d = 4 Å), EDDT (2d = 8.8 Å), and KAP (2d = 26.6 Å). Only spectrometers using the first two crystals were flown on *OSO-4*; the KAP spectrometer was added to the spectrometer package for *OSO-6*. The detectors were Ar-filled, halogen quenched Geiger-Mueller counters with mica windows. An aluminized Mylar filter was used in each spectrometer to eliminate contamination by ultraviolet radiation. The scan time for a high resolution spectrum was 13 minutes. The field-of-view was the entire Sun but the emission in these short wavelength X-ray regions is due primarily to flares, and flares occupy only a small region of the total solar disk. Thus, spectral blurring due to source size or multiple sources was not a problem for intense flares. *OSO-4* was launched in October 1967 and *OSO-6* was launched in August 1969 (see Meekins, et al. 1968).

X-ray solar flare spectra below 8 Å were found to be dominated by lines of He-like and H-like ions, ranging from the solar abundant elements from O through Ni (see Figure 60s.2.6). Weak emission from lines of He-like ions from non-abundant elements like Mn and K were also seen (see Figure 60s.2.7). In addition, between about 8 and 21 Å there are a host of Fe lines that arise from transitions between the M and L shells. The close bunching of lines due to transitions in ions such as Fe XIX were not resolvable with the spectrometers on the *OSO* satellites, but at NRL a collaboration was established by Dr. George Doschek (NRL) with Dr. Robert Cowan, a theoretical atomic physicist at the Las Alamos Scientific Laboratory and theoretical wavelengths were calculated for many of the unresolved multiplets. After Uri Feldman joined George Doschek at NRL a foundation at NRL was laid for making significant contributions towards understanding the then uncharted territory of the spectroscopy of highly ionized ions, not only in the X-ray region but throughout the ultraviolet and extreme ultraviolet spectral regions. This work was helped considerably by the laboratory spectroscopy work conducted by Feldman, Doschek, and later John Seely (NRL) and Charles Brown (NRL) that is discussed in a separate chapter of the SSD history on laboratory spectroscopy (i.e., Essay 70.5).

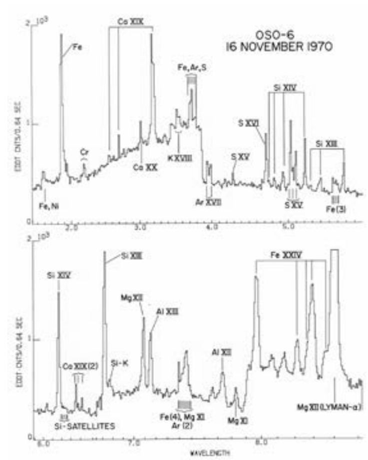

Figure 60s.2.6 – A solar flare spectrum obtained from NRL's EDDT spectrometer on OSO-6. The spectrum is not corrected for instrumental effects, i.e., the continuum edges near 4, 6.5, and 8 Å are instrumental. The wavelength glitch near 6.5 Å is due to rastering of the Harvard College Observatory EUV imaging spectrometer. When the pointing of the instrument returned to the raster start position, it produced movement that briefly affected the Bragg spectrometers (credit: NRL/NASA).

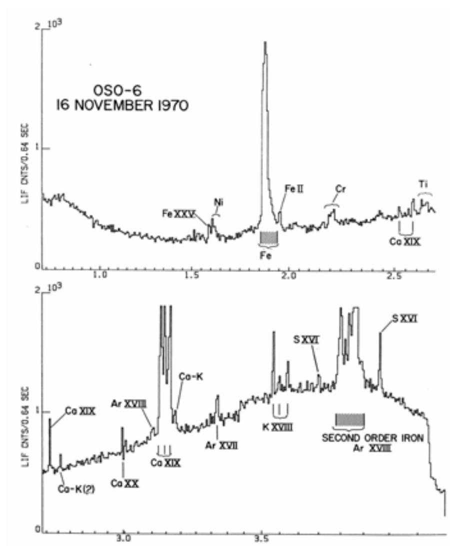

Figure 60s.2.7 – A solar flare spectrum obtained by NRL's LiF spectrometer on OSO-6. Note the He-like triplets for Ca XIX and K XVIII and the weak emission due to non-solar-abundant elements of K, Ti, and Cr. The second order region of the blended iron-line emission near 1.85 Å is starting to resolve the complex although there is blending due to the Lyman-α line of Ar XVIII (credit: NRL/NASA).

The weak emission features due to K, Ti, and Cr in Figure 60s.2.7 are spectroscopically identical to the Ca and Fe features. Thus the figure shows immediately in a qualitative manner how much less abundant K, Ti, and Cr are on the Sun compared with Ca and Fe. The figure is also misleading in this regard because the Ca lines look stronger than the Fe lines. This is due mostly to the electron temperature of the flare. Flares do not usually exceed about 25 million degrees K in temperature, and Fe XXV has not reached its maximum ion abundance at these relative "low" temperatures. But Ca has reached maximum abundance and it is therefore the ion fraction of Ca that is more abundant than the Fe abundance fraction, and not the element abundance.

Another interesting feature in Figure 60s.2.7 is the weak emission labeled Fe II. With *OSO-6* it was discovered that the Fe II emission is produced by fluorescence from the photosphere, i.e., the coronal X-rays from the flare innershell ionize the Fe in the photosphere and this produces a fluorescent glow from an extended photospheric region (Doschek, et al. 1971). The feature disappears for limb flares, which is the telltale sign that emission is due to fluorescence.

One issue plaguing interpretation of the lower resolution blended line features in the *OSO* spectra at wavelengths shorter than 4 Å was how many ions of say, Ca, or Fe, were due to emission from lines of the He-like ion and how many were due to innershell transitions in lower ionization stages. For Ca most of the emission is He-like, but as the nuclear charge increases the contributions of satellite lines formed mostly by dielectronic recombination greatly increases. The Fe feature contains emission lines from about Fe XX through He-like Fe XXV. The dielectronic lines turned out to be excellent plasma diagnostics. This was all resolved in the 1980s by instrumentation on the NRL *P78-1* spacecraft (see chapter in this history on the *P78-1* mission), the NASA *Solar Maximum Mission*, and the Japanese *Hinotori* spacecraft. Very high resolution spectrometers were flown on all three missions and the X-ray region below 21 Å was completely resolved and is now well-understood (see Figure 60s.2.8. Even without high spectral resolution, interesting results concerning flares were found from the *OSO* spectra, e.g., flare spectra were found to be multithermal, and possible density diagnostics were identified (Doschek, Meekins, & Cowan 1973).

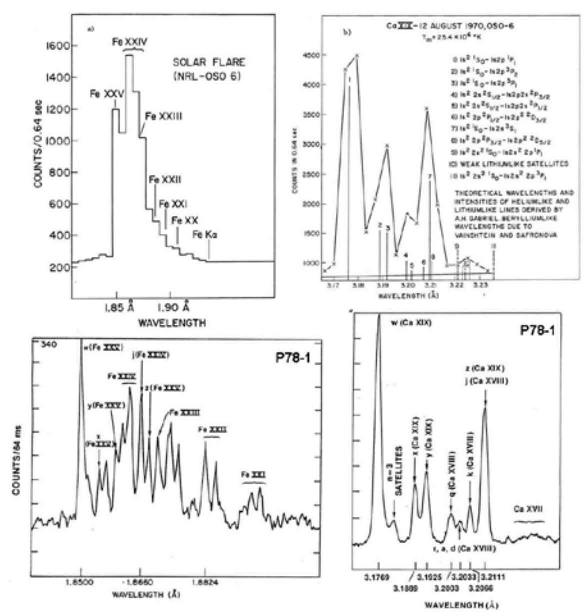

Figure 60s.2.8 – Top: Flare spectra of He-like iron (Fe XXV) and calcium (Ca VIII) and associated dielectronic satellites as resolved by the LiF spectrometer on OSO-6. Bottom: the full spectral resolution of these complex spectral regions achieved by NRL's Ge spectrometers on P78-1 flown a decade later than OSO-6 (credit, top left image: from Figure 2 in Doschek & Feldman 1976, Astronautics & Aeronautics, Vol. 14, July/August, page 24, courtesy American Institute of Astronautics & Aeronautics; top right image: NRL/NASA; credit, bottom images: from Figure 4 in Doschek 2006, Advances in Space Research, 38, 1482.)

At the time of the *OSOs*, NRL including both Tousey and Friedman had stiff competition in spectroscopy from Culham Research Laboratory in the UK and from the Institute for Spectroscopy in Moscow. At Culham now world-famous scientists like Brian Fawcett, Carole Jordan, and Alan Gabriel were making seminal contributions to the field. NRL**,** with the addition of young staff members**,** quickly caught up and made major contributions towards understanding the solar spectrum through the 1970s, 1980s, and 1990s (see Essays on the *P78-1* mission, the *Yohkoh* mission, the *Hinode* mission, and the laboratory spectroscopy work).

In summary, the NRL *OSO* Bragg crystal spectrometer experiments were among the first to investigate the detailed spectrum of solar flares and served as NRL's foundation for more powerful future investigations into solar flare X-ray emission. A review of the state of solar Bragg crystal spectroscopy in the *OSO* era is available (Doschek 1972).

References: The Orbiting Solar Observatories (OSOs)

Doschek, G. A. 1972, Space Science Reviews, 13, 765

Doschek, G. A., & Feldman, U. 1976, Astronautics & Aeronautics, 14, 24.

Doschek, G. A., Meekins, J. F., & Cowan, R. D. 1973, Sol. Phys., 29, 125

Doschek, G. A., Meekins, J. F., Kreplin, R. W., Chubb, T. A., & Friedman, H. 1971, ApJ, 170, 573

Koomen, M. J., Detwiler, C. R., Brueckner, G. E., Cooper, H. W., & Tousey, R. 1975, Applied Optics, 14, 743

Koomen, M., Howard, R., Hansen, R., & Hansen, S. 1974, Sol. Phys., 34, 447

Meekins, J. F., Kreplin, R. W., Chubb, T. A., & Friedman, H. 1968, Science, 162, 891

Tousey, R. 1973, Space Research XIII, Vol. 2, 713

60's.3: The NRL Solar Radiation (SOLRAD) Satellite Program

Contributed by George A. Doschek

1.0 Introduction

From the earliest days of space research at NRL there was a strong interest in the Sun's influence on the Earth's atmosphere, particularly the ionosphere. Solar flares were thought to be the culprits that produced communications problems involving the ionosphere. There were many questions, such as what radiation from the Sun causes the ionospheric disturbances, e.g., X-rays or perhaps UV radiation, and where does this radiation come from in the solar atmosphere. Solar physics was a highly military relevant discipline because of the effect of the Sun's radiation on the ionosphere and consequent effect on military communications. Solar physics has become more relevant because of the enormous increase of orbiting spacecraft and our practical reliance on them, including both military and civilian systems. In the Division, rockets, and balloon/rocket combinations were launched in order to make solar measurements. A spectacular Division adventure was the 1958 eclipse expedition to Pukapuka, a small coral atoll in the Danger Islands in the South Pacific. Nike-Asp rockets were launched by Division personnel led by Herbert Friedman from a Navy vessel at the time of the eclipse and showed that X-rays were associated with active regions and the emission extended beyond the white light solar disk.

All the solar observations in the 1950s indicated the need for constant monitoring of the Sun's radiative output. In the late 1950s NRL conceived of the Solar Radiation (*SOLRAD*) program, which consisted of a series of satellites dedicated to solar observations. *SOLRAD* 1 was launched in June 1960, and 10 more *SOLRAD*S were built by NRL and launched through 1976. The first *SOLRAD* was also the world's first orbiting astronomical observatory (see Figure 60s.3.1).

SOLRAD 1 was launched from Cape Canaveral on a Thor rocket and weighed 19.05 kg. Its orbit was highly elliptical, varying between 614 km (periapsis) and 1,061 km (apoapsis), with a period of 101.7 minutes and an inclination of 66.7 degrees. It monitored solar X-ray radiation between 2 and 8 Å and UV radiation between 1050 and 1350 Å (covering the important emission line of hydrogen (Lyman-α) at 1215 Å) using ion chamber photometers. Herbert Friedman**,** the Division's third Superintendent**,** was the Principal Investigator. All the *SOLRAD* spacecraft were built at NRL by what is now called The Naval Center for Space Technology (Code 8000).

Figure 60s.3.1 – The first SOLRAD spacecraft (credit: NRL).

2.0 The *SOLRAD* Spacecraft Series

The scientific value of a continuing series of solar monitoring spacecraft is that a large database is eventually obtained which allows the statistical analysis of transient events such as flares and is a record of long-term changes in solar radiative output. The *SOLRAD* series was highly successful in achieving the above goals after experiencing a difficult time between the launch of *SOLRAD* 1 and *SOLRAD* 7. The *SOLRAD* series of launches is given in Table 1, obtained from the NRL's Naval Center for Space Technology, modified by information in the NASA National Space Science Data Center (NSSDC). As mentioned, all the *SOLRAD* spacecraft were built by Code 8000 at NRL, but the solar science instruments were built in what is now Code 7600, the NRL Space Science Division. The useful period of solar monitoring is from ~1964 to ~1978. Solar monitoring continues to this day. Observations in two spectral bands, 0.5 – 4 and 1 – 8 Å, were begun in 1974 with the launch of the *Geostationary Orbiting Environmental Satellites* (*GOES*) by the National Oceanic and Atmospheric Administration's (NOAA) Space Weather Prediction Center and when combined with the *SOLRAD* data have produced a nearly continuous record of solar flare activity for more than 40 years (1969 – 2013). Recently, Neupert (2011) has inter-calibrated the soft X-ray band measurements from *SOLRAD* 9 through *GOES* 12.

Table 60s.3.1

	Launch Date	Launch Vehicle	Useful Life	Comments
SOLRAD 1	22 June 1960	Thor Able Star	10 months	First solar satellite
	30 November 1960	Thor Able Star	-------	Launch vehicle failed
	29 June 1961	Thor Able Star	5 months	Separation failed
	24 January 1962	Thor Able Star	-------	Launch vehicle failed
	26 April 1962	Scout	-------	Launch vehicle failed
	15 June 1963	Thor Agena	67 days	Orbit decayed
SOLRAD 7A	11 January 1964	Thor Agena	23 months	Operation satisfactory
SOLRAD 7B	9 March 1965	Thor Agena	52 months	Operation satisfactory
SOLRAD 8	19 November 1965	Scout	24 months	50% satisfactory
SOLRAD 9	5 March 1968	Scout	6 years	Operation satisfactory
SOLRAD 10	8 July 1971	Scout	7 years	Operation satisfactory
*SOLRAD*11A,B	15 March 1976	Titan IIIC	40 months	Operation satisfactory

The instrumentation on the *SOLRAD*s gradually grew more sophisticated and the spacecraft became larger. For example, *SOLRAD* 9 had 14 detectors that covered the ranges 20 – 80 keV, 0.5 – 60 Å, and 1080 – 1350 Å. *SOLRAD* 1 had only 3 detectors. *SOLRAD* 9 weighed 198 kg, 10 times more than *SOLRAD* 1. The two *SOLRAD* 11 spacecraft were even more sophisticated. In addition to the usual X-ray and UV monitors, *SOLRAD* 11 contained solar wind, proton and electron monitors, X-ray monochromators, solar flare polarimeters, and a cosmic X-ray background experiment. However, each spacecraft weighed less than *SOLRAD* 9, i.e., 102.15 kg. The spacecraft looked much different than *SOLRAD* 1 (see Figure 60s.3.2).

Key *SOLRAD* monitoring for solar flares were the X-ray fluxes in the 0.5 – 3, 1 – 8, and 8 – 20 Å channels. In addition to what can be learned about flares directly from the *SOLRAD* data, the data are useful as context data for other more sophisticated solar flare instrumentation.

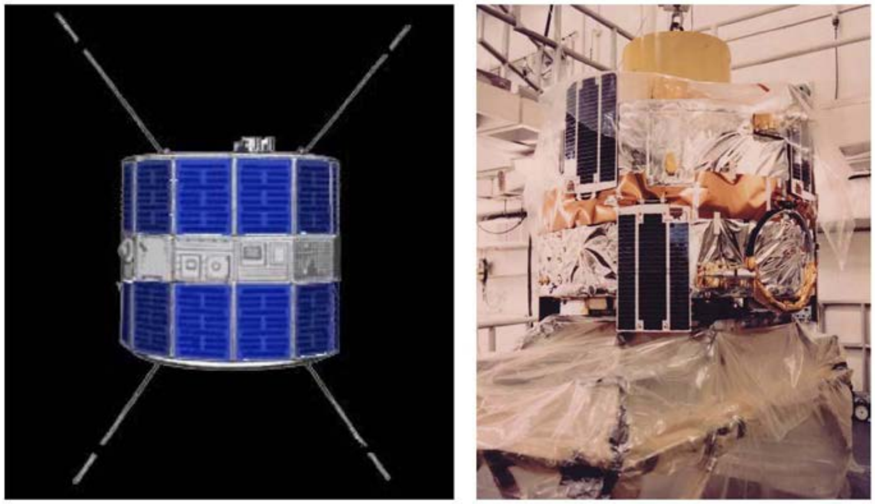

Figure 60s.3.2 – The SOLRAD 9 and 11 spacecraft (credit: NRL).

3.0 Science Results from *SOLRAD*

SOLRAD and other observations showed that solar flares have characteristic X-ray light curves such as shown in the top-left schematic graph in Figure 60s.3.3. There is usually a rapid rise in X-ray flux (between 1 minute and maybe 30 minutes) followed by a slower decay that can be as short as a minute and as long as a day. *SOLRAD* gave us some of the most basic information about these soft X-ray fluxes. In addition there is usually a hard X-ray component that appears during the soft X-ray rise phase, indicating the production of non-thermal energetic particles. We now understand (bottom-left, Figure 60s.3.3) that the soft X-ray emission arises in closed magnetic flux tubes (not observable with *SOLRAD*) and there are theories explaining the onset of flares via the process of magnetic reconnection that is believed to occur above these closed flux tubes. Theoretical models describe the tubes as being filled with hot plasma by chromospheric evaporation due to energy input from the reconnection region (lower-right, Figure 60s.3.3).

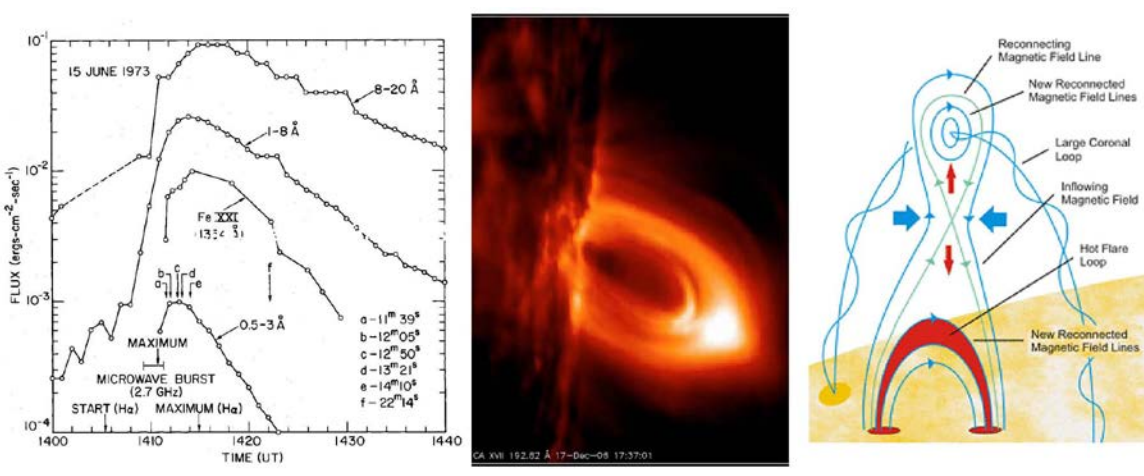

Figure 60s.3.3 – Left: SOLRAD data in action, here used as context data for NASA Skylab mission data (see Skylab Essay in this history); middle: images of flare loops obtained from the Extreme-ultraviolet Imaging Spectrometer (EIS) instrument on Hinode launched in 2006 (see Hinode Essay in this history); right: schematic theoretical diagram of a flare (credit left image:Figure 1 in Doschek, Feldman, & Rosenberg 1977, reproduced by permission of the AAS; middle image, NRL/NASA; right image, NASA)

Some specific science results from *SOLRAD* are:

- From *SOLRAD* 1: Data confirmed the hypothesis that Sudden Ionospheric Disturbances (SIDs) are caused by solar flare X-ray ionization of the D region, and not by UV Lyman-Å radiation. SID phenomena occur when the solar X-ray flux below 8 Å exceeds 2 x 10^{-8} ergs/cm^{-2}/s above the Earth's atmosphere (Kreplin, Chubb, & Friedman 1962).
- Using *SOLRAD* 10 data, a detailed quantitative investigation of the temperature distribution of flares indicated that the 0.5 – 60 Å flare radiation could be explained by purely thermal processes (Dere, Horan, & Kreplin (1974). The low-energy cutoff energy for the production of non-thermal electrons is still not known (see Figure 60s.3.4).
- The behavior of extreme-ultraviolet emission and impulsive hard X-ray emission was also related to soft X-ray flare emission, a result important for space weather as the observations encompassed the entire Sun (Horan & Kreplin 1981; Horan, Kreplin & Fritz 1982; Horan, Kreplin, & Dere 1983). These observations were obtained from *SOLRAD* 11 and are among the most comprehensive UV-X-ray wavelength coverage of flares yet obtained (see Figure 60s.3.5).
- The *SOLRAD* data have been used in many papers as context data in the analysis of data from other instruments. An example is shown in the top-right panel of Figure 60s.3.3 from Doschek, Feldman, & Rosenberg (1977). In the Doschek et al. paper, the main focus is the analysis of flare spectra from the NRL S082-B slit spectrograph on the *Skylab* manned space station. The *SOLRAD* data were useful in showing the authors at what time in the typical flare evolution their spectra were obtained. This type of work is still common using data from *GOES* spacecraft.

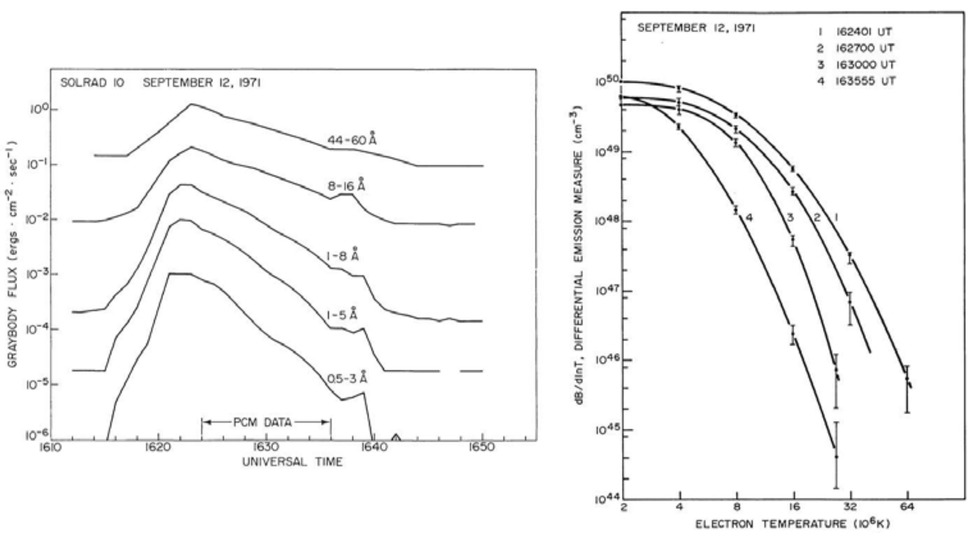

Figure 60s.3.4 – SOLRAD 10 fluxes used to compute a differential emission measure for a flare (credit: Figures 2 and 3 in Dere, Horan, & Kreplin 1974, courtesy Solar Physics).

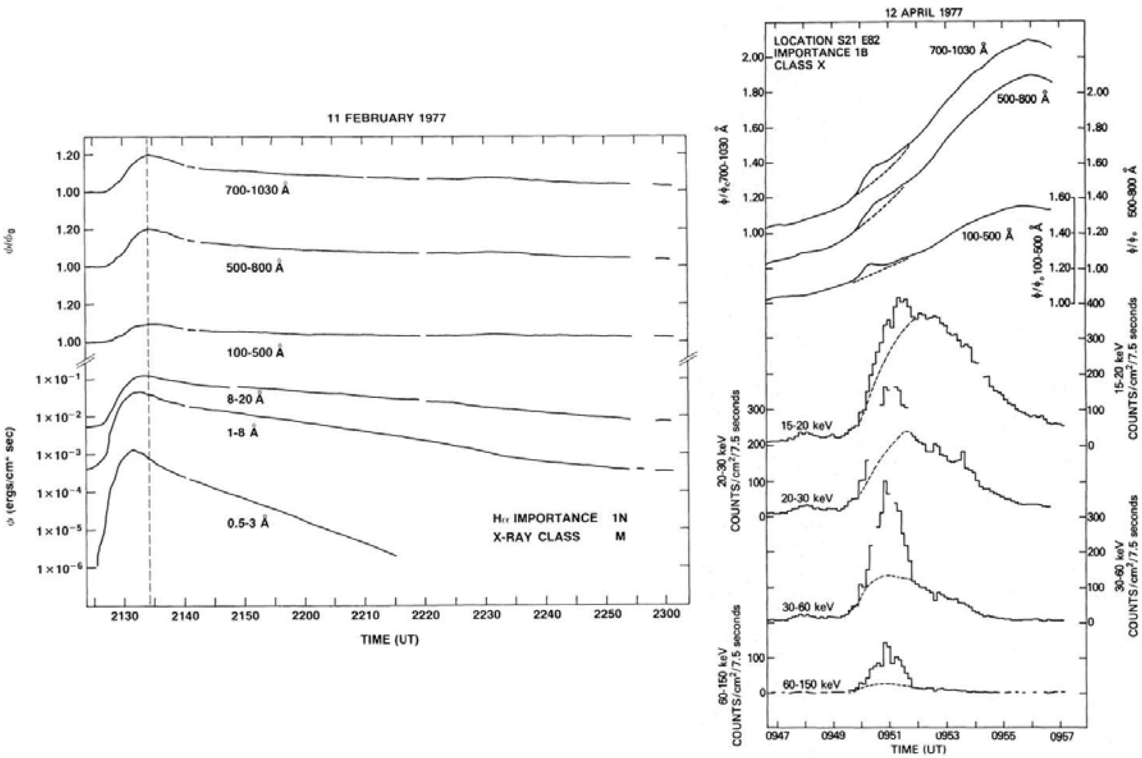

Figure 60s.3.5 – Impulsive and gradual flare radiation from the UV to hard X-rays. Left: Figure 3 in Horan & Kreplin (1981), courtesy Solar Physics; Right: Figure 2 in Horan, Kreplin, & Fritz (1982), reproduced by permission of the American Astronomical Society. The dotted lines in the right-side figure are estimates of the gradual component. The vertical dotted line in the left-side figure is a good reference for seeing how the peak emissions in different wavelength regions are related. The most energetic emission always peaks first, indicating that the flare temperature peaks before the flare fluxes. From NRL instruments on OGO-4, Horan (1971) showed that typically the flare temperature (from 0.5 – 3 and 1- 8 Å fluxes) peaks first, the 0.5 – 3.0 Å X-ray flux peaks second, and the emission measure determined from the X-ray fluxes peaks last.

In summary, the *SOLRAD* spacecraft initiated a giant step forward in astrophysical research from space in showing the great value of continual observations of astrophysical sources over many years. The solar data from the spacecraft also provided an in-depth look at high energy flare radiation for many different types of flares. Knowledge gained from SOLRAD is fundamental for an understanding of the causes of space weather that are a continuing concern for our modern space-based technology.

It is also interesting to note that the *SOLRAD* 11, also known as *SOLRAD HI*, launched in 1976, participated in NASA operations in addition to purely solar physics science. *SOLRAD* 11A lasted 15 months and 11B lasted 40 months. The goal of the operations project was to provide to NASA's astronauts an almost instantaneous warning of any solar event that might harm them so they could take protective measures. The way this was accomplished was by maneuvering the two satellites (*SOLRAD* A & B) into very high orbits (60,000 NM circular and separated by 180 degrees) so that at least one satellite would always be in view of the Sun. Thus any major solar event could be instantaneously radioed to NASA to warn the astronauts.

George Doschek thanks NRL's Peter Wilhelm**,** Director of the Naval Center for Space Technology**,** for reviewing and adding material to this essay.

References: The NRL Solar Radiation (SOLRAD) Satellite Program

Dere, K.P., Horan, D.M., & Kreplin, R.W. 1974, Solar Phys., 36, 459

Doschek, G.A., Feldman, U., & Rosenberg, F.D. 1977, ApJ, 215, 329

Horan, D.M., 1971, Solar Phys., 21, 188

Horan, D.M., & Kreplin, R.W. 1981, Solar Phys., 74, 265

Horan, D.M., Kreplin, R.W., & Dere, K.P. 1983, Solar Phys., 85, 303

Horan, D.M., Kreplin, R.W., & Fritz, G.G. 1982, ApJ, 255, 797

Kreplin, R.W., Chubb, T.A., & Friedman, H. 1962, JGR, 67, 2231

Neupert, W.M. 2011, Solar Phys., 272, 319

60's.4: Rocket Astrophysics: 1960's, 1970's, and Beyond

Contributed by Michael P. Kowalski, Kent S. Wood,
and Gilbert G. Fritz, *retired from NRL*

1.0 Introduction

The dawn of the space age made possible investigations of astronomical sources at wavelengths previously unobservable because the radiation is absorbed by the Earth's atmosphere. Rocket measurements at NRL began with Dr. Herbert Friedman, the Division's third Superintendent, and colleagues using captured V-2 rockets initially and then Viking, Deacon, and Aerobee sounding rockets to launch simple but technically innovative UV and X-ray instruments. This work concentrated on atmospheric and solar physics and has been summarized in an internal technical report for the period 1946-1957.[1] Section 2 below describes some highlights and their impacts. Prior to satellites dedicated to astronomy, rockets provided the dominant path to space-based measurements. Discovery of X-rays from the Sun (1949) led to further solar flights. Extra-solar X-ray astronomy started in in the early 1960s and is the principal subject of this chapter. X-ray work after 1985 at NRL was entirely from satellites and is treated elsewhere in this history but a new phase of high resolution EUV spectroscopy began in the 1990s with flights down to the present and these are described here. This chapter omits astrophysics flights whose aim was to conduct infrared measurements (although there was a program of that nature, initially led by Martin Harwit, Cornell University) nor does it cover UV rocket flights in the half century from 1950 to 2000 that is related to work described in Sec. 60's.2, except insofar as they provide background to how the X-ray activity began.

The early years were a time of great excitement and discovery for rocket astrophysics; see, e.g. Table 60s.4.1. Virtually all astronomical sources known up to that time (e.g., white dwarfs, normal and active stars, supernovae remnants, clusters of galaxies) were unexpectedly found to produce X-ray radiation, and new classes of objects (e.g., neutron stars, black holes) were discovered. Theoreticians scrambled to explain the new observations, which were driven by radical advances in instrumentation. Friedman[2] captures the essence of these times:

"My colleagues were all physicists; none of us had been exposed to formal education in astronomy. Astronomers at the time were busy pursuing studies with ground-based telescopes, and shunned the electronic gadgetry, radio telemetry, and especially the risks associated with rockets. It took an adventurous breed of scientist to spend months to a year preparing a payload that would be perched atop a huge rocket motor, suffer a violent shock upon takeoff, and disappear into the blue yonder....The tension of the countdown, and apprehensions about malfunctions after the launch, when there was no recourse, were enough to discourage faint-hearted souls….In spite of forbidding odds, high-altitude research with rockets provided dramatic mixtures of exaltation and trauma for early practitioners, a sense of high adventure, of bold gambling with big stakes and great risks. We would flirt with disaster while anticipating unexpected discoveries from exploration of unknown regimes…"

Table 60s.4.1. Principal extra-solar X-ray and EUV rocket flights of NRL

Mission	Date	Range	Instrument	Science Result
	Apr 1963	WSMR	Collimated X-ray Geiger counter (CGC)	• Detection of First-discovered Extra-Solar X-ray Source Sco X-1 • Detection of Crab Nebula X-ray emission
	Jun 1964, Nov 1964	WSMR	CGC	• Discovery of 8 new X-ray Sources in Taurus, Cygnus, Ophiuchus, Sagittarius, Serpens
	Jul 1964	WSMR	CGC	• Crab Lunar Occultation: Search for Crab pulsar, Extent of nebular X-ray emission
	Apr 1965	WSMR	CGC	• Discovery of X-ray emission from Cas-A & M87 (Virgo cluster)
	May 1967	WSMR	Collimated X-ray proportional counter (CPC)	• Discovery of X-ray emission from 3C 273 • Detection of M87 X-ray emission
NB 3.196 (NB=Navy) Aerobee	Sep 1967	WSMR	CPC	• Spectra of Sco X-1, Cyg X-1, Cyg X-2 • Variability in Cyg X-1 and in Cygnus Loop • Spectrum of Hot Intergalactic Medium near Galactic Pole
	Apr 1968	WSMR	CPC	• Detection X-rays from radio galaxy Cen A
NB 3.210 / NASA 4.290 Aerobee	Mar 1969	WSMR	CPC	• Detection of Crab Nebula Pulsar • Spectra of Crab Nebular and North Galactic Pole • Discovery of X-ray emission from Coma Cluster
NB 3.237 Aerobee	Mar 1970	WSMR	CPC + UV Geiger counters	• Discovery of X-ray emission from Perseus cluster • Diffuse X-ray and UV Spectra in galactic anti-center
NB 4.244 Aerobee	Nov 1971	WSMR	CPC	• Possible Detection of Supernova in North Polar Spur • Scan of Crab, Detection of supernova remnant in IC443
NB 4.257 Aerobee	Oct 1972	WSMR	CPC	• Complement NB 3.237 diffuse survey • Detection of supernova remnant in Eridanus
NASA 13.091 Aerobee	Apr 1973	WSMR	CPC	• Low-energy X-ray pulses from Her X-1 during ON-state • Confirm supernova origin of X-ray source in North Polar Spur
NASA 13.100 Aerobee	Nov 1973	Woomera	CPC	• Detection of pulsed X-ray emission from SMC X-1
NASA 26.025 Aerobee	Sep 1974	WSMR	CPC	• Low-energy X-ray pulses from Her X-1 during OFF-state • Detection of X-rays from Cygnus supernova remnant
NB 24.275 Aries	Dec 1974	WSMR	CPC	• Intended Target: Crab Lunar Occultation • Launch Failure: Aries blew up at T+58 sec
Apollo-Soyuz MA-048	Jul 1975	Orbital	CPC + EUV instrument	• Detection of pulsed X-ray emission from SMC X-1 • Detection of X-rays from MSH 14-63 supernova remnant • Detection of X-rays from Coma cluster • X-ray upper limit on white dwarf HZ 43 (EUV detection)
NASA 26.047 Aerobee	Oct 1975	WSMR	CPC	• Intended Target: Galactic center • ACS Failure: Rocket did not point at intended targets.
NASA 26.049 Aerobee	Apr 1976	WSMR	CPC	• Scanned Galactic center: resolved *Uhuru* extended source into 4 point sources
NASA 26.052 & 26.053 Aerobee	Feb 1977	Woomera	CPC	• Structure and extent of Coma cluster X-ray gas • Detected 3 new X-ray source in LMC bar, one associated with supernova remnant N132D
NASA 27.035 Black Brant (BB)	Sep 1980	WSMR	Imaging Mirror (IM) + MCP detector	• Intended Targets: Cyg X-1, Cas A supernova remnant • Technology Demonstration Successful • ACS Failure: Rocket did not point at intended targets
NASA 27.009 BB	Nov 1981	WSMR	IM + Imaging Proportional Counter: *ROSAT* prototype	• Cyg X-1, Cas A supernova remnant • Technology Demonstration Successful
SPARTAN-1 NASA STS-51G SpaceShuttle Discovery	Jun 1985	Orbital	CPC	• Tomographic maps of Galactic center: Detected 5 point sources (one new) and diffuse source with 2 embedded point sources • Tomographic X-ray map of Perseus cluster: morphology and mass of diffuse X-ray gas out to 1.6 Mpc • Discovered radial gradient in Fe-line in Perseus cluster
NASA 36.162 BB	Feb 2000	WSMR	*J-PEX*	• Intended Target: White Dwarf G191-B2B • Failure to correctly evaluate winds: Payload cut down
NASA 36.195 BB	Feb 2001	WSMR	*J-PEX*	• First high-resolution EUV spectrum on non-solar object: the Isolated White Dwarf G191-B2B: photospheric & ISM He II
NASA 36.207 BB	Oct 2008	WSMR	*J-PEX*	• High-Resolution EUV Spectrum of Binary White Dwarf Feige 24: photospheric and ISM He II

Missions were initially sponsored by ONR/NRL and launched under the Navy program at the White Sands Missile Range (WSMR; Fig. 60s.4.1.1). However, NASA participation grew eventually from a joint venture with the Navy in 1969 to dominate sponsorship and launch management. One benefit from NASA support was access to their launch capabilities in Woomera Australia (Fig. 60s.4.1.2), where southern hemisphere astronomical targets could be observed. In the above table, references are keyed to mission number or to date flown by the Space Science Division (SSD). The Division existed only after 1952 and earlier flights discussed in Section 2 were carried out by Divisions from which the Division that is the subject of this work was formed. We have selected several important missions for further discussion. While NRL enjoyed a mission success rate much higher than other research groups, the table shows it was not flawless. The Aerobee (Nike-boosted) sounding rocket was the workhorse launch vehicle in the 1960s giving way later to the (Terrier-boosted) Black Brant (BB), thus gradually increasing apogees and observation times up to their present values of several hundred kilometers and slightly over five minutes, respectively. The successful return of the payload by parachute allowed for instrument upgrades and re-flights (note in the table the back-to-back missions, 26.052 and 26.053, flown one week apart using the same payload). Early instruments were simple X-ray Geiger counters, but this evolved rapidly to large-area (Collimated) X-ray Proportional Counter detectors (CPCs, Fig, 60s.4.1.3) that filled the available rocket volume and weight-lifting capability (important limitations even today). Some missions were ambitious (e.g., NB 3.237) having both X-ray and UV instruments. Observations were pointed or scanned, the latter sometimes obtained by spinning the rocket along its axis. Rocket pointing information was combined with the detector's collimated field of view (~few degrees) to crudely locate the X-ray source (Fig. 60s.4.1.4, but see section 3.0), to be identified astronomically by cross-correlating with higher-resolution positions found in catalogs made at other wavelengths (e.g., visible, radio).

Figure 60s.4.1.1 - Mission 36.207: WSMR, Oct 2008 (clockwise from upper left): (a) Payload test on launch rail, (b) Launch, (c) Helicopter return of payload, over White Sands Monument, and (d) Recovery on flatbed truck (center: Kowalski, right: Cruddace, credit: WSMR).

Figure 60s.4.1.2 - Mission 13.100: Woomera, Australia, Nov 1983 (left) Payload being assembled and (right) Launch pad. Arid conditions, sparse vegetation, and low population density are common to land-based sounding rocket ranges (credit: NRL).

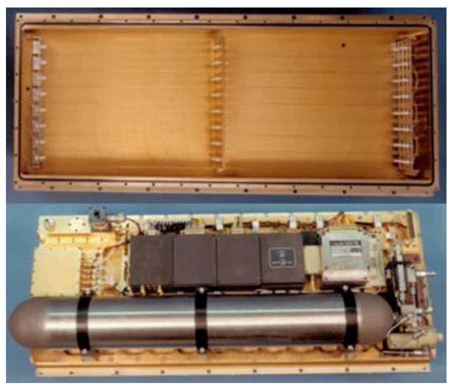

Figure 60s.4.1.3 - Proportional Counter: (Top) Rectangular box encloses gas on five sides and contains HV anode wire grid. View is from the remaining side that encloses the gas with a thin-film X-ray window (removed). (Bottom) Box rear contains electronics and the gas handling system; the cylinder is the gas reservoir (credit: NRL).

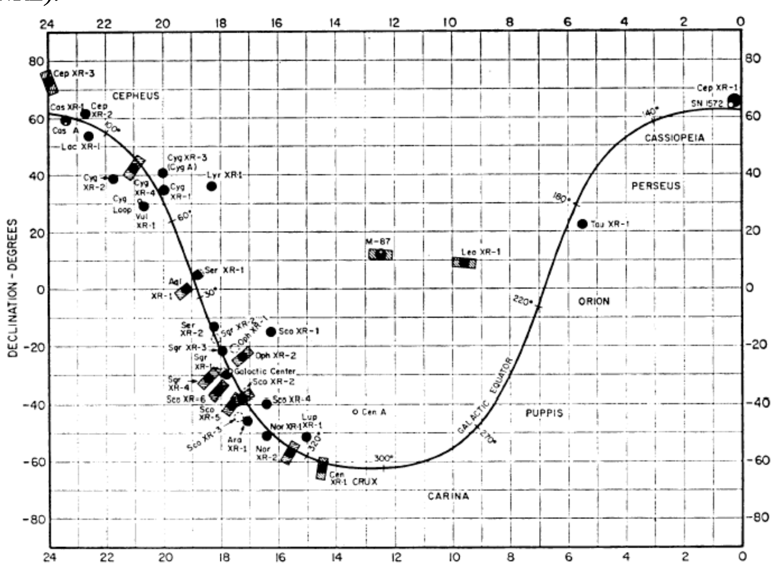

Figure 60s.4.1.4 - Mission Apr 1965 (Friedman et al. 1967): Map of X-ray sources detected in NRL rocket surveys of 1964 and 1965. Estimated uncertainties in source positions are generally 1.5º. Shaded rectangles indicate 4º pitch uncertainties detected on only one roll scan (credit: NRL).

As a general procedure, survey flights discovered celestial X-ray sources, then further flights were made on selected bright sources to characterize properties and thereby model and understand the exciting physics occurring within. Conditions (e.g., densities, temperatures, abundances, magnetic fields) in astronomical X-ray sources are either not reproducible on Earth, thus providing insight into basic physics, or involve high energy plasma processes that have Navy relevance in fields such as fusion power. The workhouse instrument, the CPC, allowed measurements of (a) the spatial structure of extended sources (e.g., nearby galaxies, supernova remnants, and clusters of galaxies), (b) temporal variability of non-extended (point) sources such as in stellar coronae and in condensed matter objects (white dwarfs, neutron stars, and black holes), any of which might be in binary systems thus producing periodic emission, and (c) low-resolution spectra. While the only line detectable was the complex of hydrogenic Fe at ~6 keV, the overall spectral shape provided critical constraints on source emission models and on properties of the intervening Interstellar Medium (ISM). An additional fundamental discovery in 1956 was the existence of an isotropic X-ray background[3-6] spanning the entire sky with both galactic and extragalactic contributions. Resolving weak but discrete sources from the background (Fig. 60s.4.1.5) and characterizing the spectrum of the remaining diffuse component (Fig. 60s.4.1.6) was a subsequent goal.

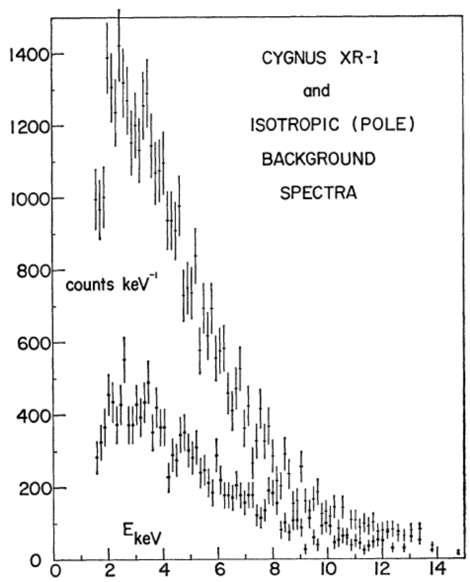

Figure 60s.4.1.5 - Mission NB 3.196 (Meekins et al. 1969): Energy spectrum of Cyg XR-1 (upper set of points) and background spectrum near galactic pole. Note that source and background intensities are comparable at the highest energies, and the spectra turn over at low energies because of ISM absorption (credit: NRL).

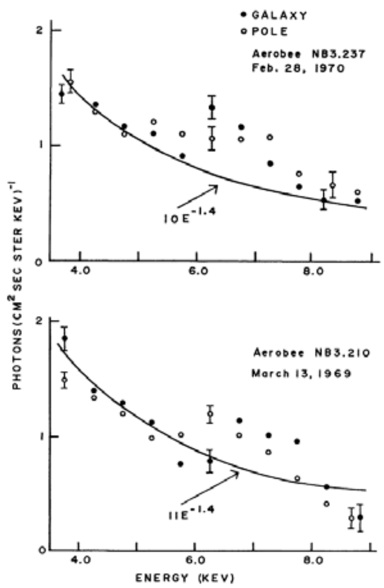

Figure 60s.4.1.6 - Missions NB 3.237 and 3.210 (Shulman et al. 1971): Spectrum of the X-ray background taken from two flights in the galactic plane (filled circles) and at the galactic pole (open circles). The smooth curve indicates a power-law spectrum, $E^{-1.4}$. Note that the bump at ~7 keV indicates (Fe-line) indicates the presence of thermal emission (credit: NRL).

Talbot Chubb was the Upper Air Physics Branch Head (Code 4120) in the Division and led the astrophysics rocket program with principle section heads being E.T. Byram and Gilbert G. Fritz (later to be the Head of the X-ray Astronomy Branch, Code 7620). They were assisted by a generation of (primarily NRL federal employee) scientists (some bringing experience at EUV and UV wavelengths) such as NRL's John Meekins, Richard (Dick) Henry, Stu Bowyer, Daryl Yentis, Seth Shulman, and Ray Cruddace as well as dedicated support engineers. The X-ray astrophysics rocket program had a parallel effort in the Division's solar physics group, described elsewhere in this history, and there was crossover in personnel (e.g., Fritz, Meekins) as well as some commonality in instrumentation and techniques.

The astrophysics sounding rocket program continues today under a new generation (e.g., Michael Kowalski) using more reliable launch vehicles and sophisticated high-resolution instruments (e.g, *J-PEX*) that better elucidate the physics on the brightest and most interesting of the astrophysical sources discovered earlier. This mode of astrophysics also serves two other critical functions. First, it is a relatively low-cost test-bed for new instrumentation, advancing technology to acceptable values for future use on larger space observatories. Second, it is a training ground for the next generation of space astrophysicists, especially instrumentalists. Several Ph.D. theses have come out of these missions, as well as early-career publications by postdocs and junior NRL staff members.

NRL was one of several groups in this new field of high-energy astrophysics from sounding rockets and competed successfully, as might be gauged by the high proportion of table references published in prestigious journals such as Science, and Nature. The following Sections further discuss selected highlights, but we begin by reviewing the developments prior to 1963 that positioned NRL to be able to do this work.

2.0 The Discovery of X-rays from the Sun and its relation to X-ray Astronomy

When Herbert Friedman shared the 1987 Wolf Foundation Prize for Physics with Riccardo Giacconi and Bruno Rossi, the citation referred to all three as principal founders of X-ray astrophysics, and Friedman in particular was cited for pioneering investigations in solar X-rays. This citation illustrates how the initial discovery of X-rays from the Sun straddles the boundary between astronomy and solar physics. This discussion will speak solely to the astronomical side of that divide because solar physics is covered in other chapters. The astronomical history is complex, but crucial to both astrophysics and NRL.

The distinction between solar physics and astrophysics is essentially artificial – the Sun is a star and from a physics standpoint the distinction derives entirely from our happening to observe the entire universe from platforms near that star. The idea that the Sun is a star has literature back to Giordano Bruno who published it in 1584. For the sixteenth century it was a breathtaking idea, even a heresy for which Bruno later paid the ultimate price. Bruno described it not only in prose but also verses that capture the first appreciation of the immensity of interstellar space in a way that anticipates science fiction. Astronomy in subsequent centuries firmly showed the Sun to be a star and diminished the novelty, hence by the V-2 sounding rocket era it was beyond doubt scientifically. Once the Sun was known to be an X-ray source the implication that other stars could be X-ray sources was inescapable. Thus one could say Friedman's discoveries of X-rays from the Sun, and later demonstration that the X-rays originate in the corona mark first detection and characterization of a member of what is now recognized as the class of coronal X-ray sources, a class that by now has tens of thousands of other catalogued members. Ergo, the first observational detection of any member of any X-ray astronomical source class is the NRL group's detection of the Sun. This viewpoint, however, is controversial because it runs against a long tradition that commences X-ray astronomy with discovery of the first extra-solar X-ray point source, Sco X-1, by American Science & Engineering's (AS&E) Giacconi, Gursky (The Division's fourth Superintendent, then at AS&E), Paolini, and MIT's Rossi, in a sounding rocket flown in 1962.[7] The strictly solar phase of X-ray research was 1949-1962, much of it dominated by NRL. Thereafter solar and extra-solar X-ray research developed in parallel.

That later discovery of the extra-Solar X-ray point source, Sco X-1 by Giacconi's group at American Science and Engineering was a dramatic event appreciated by the whole world and it was central to the course of events at NRL. Had the coronal class been all that there was to X-ray astronomy, one would have needed five to ten orders of magnitude sensitivity improvement over Friedman's rocket-borne detectors to see X-rays from coronae of even the next closest stars in the solar neighborhood. This need for vastly increased sensitivity followed directly from known distances of those stars. It stimulated efforts to develop better detectors at NRL, in Giacconi's group and elsewhere, but the outcome showed that such an extrapolation was pessimistic because of the existence of unsuspected source classes. The great surprise of Sco X-1, then, was that there are X-ray sources in our Galaxy whose intrinsic luminosities exceed the Sun's X-ray luminosity by more than ten orders of magnitude. Sco X-1 was the first discovered, hence the first of a new non-coronal class. Specifically, Sco X-1 was the first X-ray source associated with a neutron star, found years before any pulsars were known and at a time when neutron stars were still speculative. It was to take more than fifteen years to prove Sco X-1 itself was a neutron star. Clear proof that neutron stars are an X-ray class came sooner via a different source, the Crab Pulsar. This was another NRL discovery because after 1963 NRL's own pursuit of neutron star physics had begun: for this, see below, section 3 and the table, mission NB 3.210. As for the coronal source class in extra-solar X-ray astronomy, it arrived in due course when more sensitive detection systems were developed. (Note: Later NRL efforts in that area are found in essays in this history, e.g., 70s.4 HEAO-1, and describing extra-solar coronal activity on energy scales far exceeding those on the Sun.)

An equally striking aspect of the discovery by Giacconi et al. of Sco X-1 was that there existed Galactic sources prominent in X-rays but hard to detect in other wavelengths at all, in contrast to the Sun, where the discovery was seeing that star in X-rays for the first time. This leads to a different aspect of Friedman's solar discovery, namely that the possibility of detecting solar X-rays at all was still being discussed in 1949, when detection was first achieved. Work by W. Grotrian and B. Edlen during the 1940s on spectral lines of highly-ionized species detected in the corona had led to recognition that there needed to be a hot corona, with temperature estimates as high as one million Kelvin;[8] however, this had apparently not produced a prediction of observable X-ray flux. There were other schools of thought and apparently some thought the solar photosphere was too cool to emit X-rays and that temperature should only decrease going outward from the photosphere, because of the Second Law of Thermodynamics. Both X-ray and gamma-ray solar and astrophysics were years in the future in 1949 and the only known non-thermal spectra were in radio or pertained to cosmic rays. It is clear in retrospect that the Sun exhibits both hot plasmas and non-thermal spectra and is representative of the entire world of high energy astrophysics, although the neutron star and black hole sources achieve far more spectacular energy releases. In 1949, it would have required rare theoretical vision to anticipate even bits of the imminent revolution in understanding. However there was independently a strong experimental incentive to explore the Sun's spectrum to shorter wavelengths than had yet been demonstrated, with other groups competing in that pursuit. NRL had the most efficient plan for getting to that goal. The usual viewpoint is that the pivotal rocket flight was that of September 25, 1949, in which X-rays coming from the Sun were clearly detected using photon counters sensitive in X-rays and combined with filters, however that flight was preceded by two others in August, 1948, and February, 1949, in which there were hints of solar emission. Those earlier flights used, respectively, film strips and a thermo-luminescent phosphor behind a Be strip and were not regarded as sufficient.

Here is part of Friedman's (1977)[9] reminiscence of the 1949 V-2 flight that realized the goal, in which he emphasizes the ionizing effect of the solar flux on ionospheric layers and the incremental approach of coupling the X-ray detector with a UV detector that was more certain to bring results: "An opportunity to test my approach finally came in 1949, when we prepared a collection of photon counters sensitive to narrow bands of the ultraviolet and x-ray spectrum, and coupled them to radiotelemetry. The V-2 flew to 151 kilometers. […] As the radio signals came in we first read Lyman-alpha extreme ultraviolet at about 75 kilometers followed by soft x-rays above 85 kilometers. […] In one simple set of measurements we identified Lyman-alpha as the source of D-region ionization and identified soft x rays with E-region production…."

After 1963 NRL participated vigorously in the search for other celestial sources, making many first discoveries of sources and major phenomena (see Table 60s.4.1). The competition between NRL and other X-ray extra-solar groups eventually resolved itself in the succession of Herbert Friedman as SSD Superintendent by Herbert Gursky, who had been part of Giacconi's Sco X-1 team. Giacconi himself went on to receive the Nobel Prize in 2002 for pioneering contributions to astrophysics which led to the discovery of cosmic X-ray sources. The Nobel Prize citation described Friedman's role, but it was awarded two years after his death.

3.0 The Crab Nebular and Pulsar

The Crab Nebula is the remnant of a recent, comparatively nearby supernova observed in 1054 AD. It has expanded ever since and has been a prime observing target for astronomy for centuries because of the physics puzzles it presents. It is now known to consist of an energetic pulsar – the Crab Pulsar -- slowly spinning down (increasing its rotation period) by using its dipole magnetic field to accelerate particles and produce radiation. The surrounding region of particles and magnetic field is the Crab Nebula, energized by the pulsar. This characterization is partly the result of the research presently to be described, key parts of which were accomplished at NRL using a succession of X-ray payloads on sounding rockets in the 1960s launched by Friedman and collaborators. The contemporary picture of this complex source is that the Crab Nebula and the Crab Pulsar embedded in it both emit from radio to gamma-rays, but prior to the rocket work only the radio-to-optical part of the spectrum had been characterized and shorter wavelengths were terra incognita. Work on the Crab continues now, with resources such as the Fermi satellite and radio telescopes observing it regularly as new kinds of flaring and variability are monitored. An observation with the *Rossi X-ray Timing Explorer* (*RXTE*) satellite in 2011 by NRL and NASA scientists essentially repeated 1960s NRL measurements described below, but with vastly improved instrumentation to pursue more advanced ends.

Discovery of the first extra-solar source Sco X-1 (1962; see above Section) stimulated the search for other sources using detector payloads carried aloft on sounding rockets. The second one discovered was the Crab, and was found by Division researchers (Mission: Jul 1964, Bowyer et al. 1964). Thereafter the Crab became something of a specialty for NRL extra-solar X-Ray research. The next major development took place the following year, 1964, and involved using a rare celestial event, a lunar occultation, to establish the structure of the Nebula in X-rays -- but without actually imaging it in the conventional sense of that term. (X-ray optics and focusing imagery of celestial X-ray sources came more than a decade later; see section 5) In 1964 the primary question was whether the X-ray source was the Nebula or a neutron star (and neutron stars were not yet known to pulse). A lunar occultation could readily distinguish between these possibilities. In such events, which are similar to eclipses, the Moon passes between the observer (at Earth) and the source, blocking it out by sweeping in front of it. A point source (such as a neutron star) will disappear suddenly, giving a square-wave time profile, while an extended source will be eclipsed piece by piece, yielding an S-shaped curve. Formally, that the derivative of the observed temporal profile is a one-dimensional map of surface brightness, equivalent to summing the surface brightness in strips, where the strips run parallel to successive positions of the lunar limb. Lunar occultations never occur for sources more than about 6 degrees off the Ecliptic plane on the sky. The Crab is in the band where occultations are possible; events come twice per 18-year precession cycle or about every nine years. By good fortune an occultation occurred in 1964, just months after the Crab had been found in X-rays. Friedman recognized the unique opportunity and made preparations to exploit it. It was necessary to go for that opportunity or wait more than eight years. Payload preparation could not slip because the event set the schedule.

On 7 July 1964 NRL launched a sounding rocket from White Sands that carried two Geiger counter detectors. The vehicle carried the payload to a place where the lunar shadow would sweep at the apogee of the flight, and there it observed the occultation successfully. The observation was tricky because in summer the Crab is near the Sun and the timing had to be arranged so the Sun would not interfere with the intended observation. The entire flight brought wide acclaim for the elegant concept and skillful execution. More than two decades later Prof. Freeman Dyson of Princeton University wrote (Dyson 1986)[10]: “The most brilliant achievement of the sounding rocket era was Herb Friedman’s 1964 measurement of the angular size of the X-ray source in the Crab Nebula, using the moon as an occulting disk.”

The two detectors recorded similar profiles of the event. The result was that the profiles were of the S-shaped variety, which is to say the bulk of the X-ray emission (~90%) comes from the extended Nebula. Noise in the data made it impossible to see if there was any abrupt drop at the moment of eclipse of the position where a neutron star was suspected. This was before the Pulsar was known and the data lacked the time resolution needed to see its pulses. Results were published in Science (Mission: Jul 1964, Bowyer et al. 1964), describing the payload, flight, analysis, and conclusions. Fig. 60s.4.3.1 shows the light curve obtained and Fig. 60s.4.3.2 shows successive positions of the lunar limb superposed on the image of the Nebula. From the combination of the two it can be inferred that the X-ray Nebula is significantly more compact than that seen in optical.

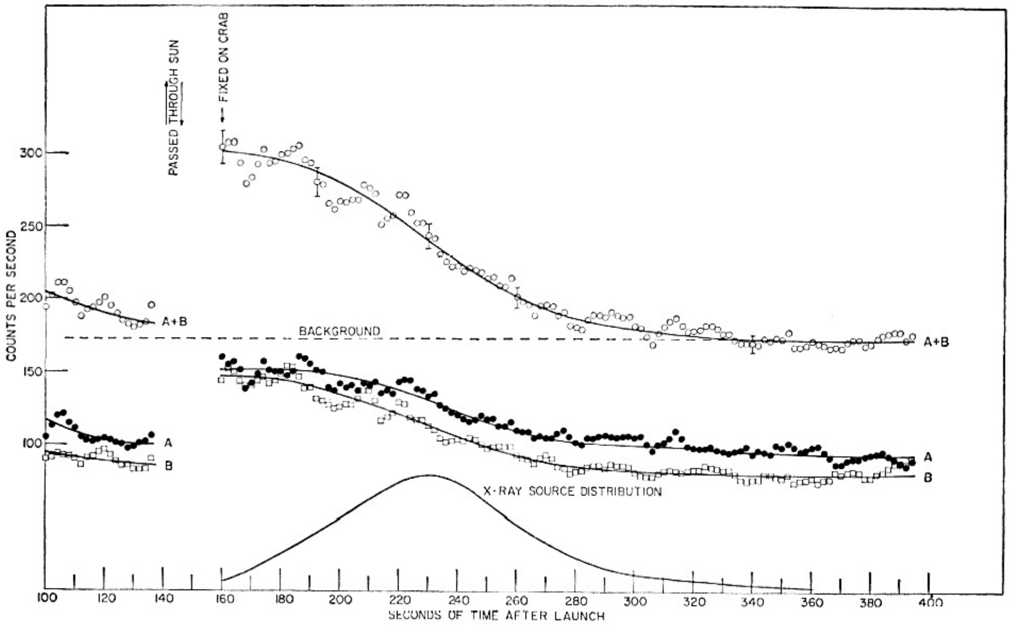

Figure 60s.4.3.1 - Variation of the observed x-ray flux during the course of flight of 7 July 1964. The Mylar windows of counters A and B were 1 mil and ¼ mil thick, respectively. Counting rates were computed from the time required for a fixed count of 768 in each counter. A running mean is plotted at 2-second intervals. The x-ray source distribution is the derivative of the A and B curve (credit: NRL).

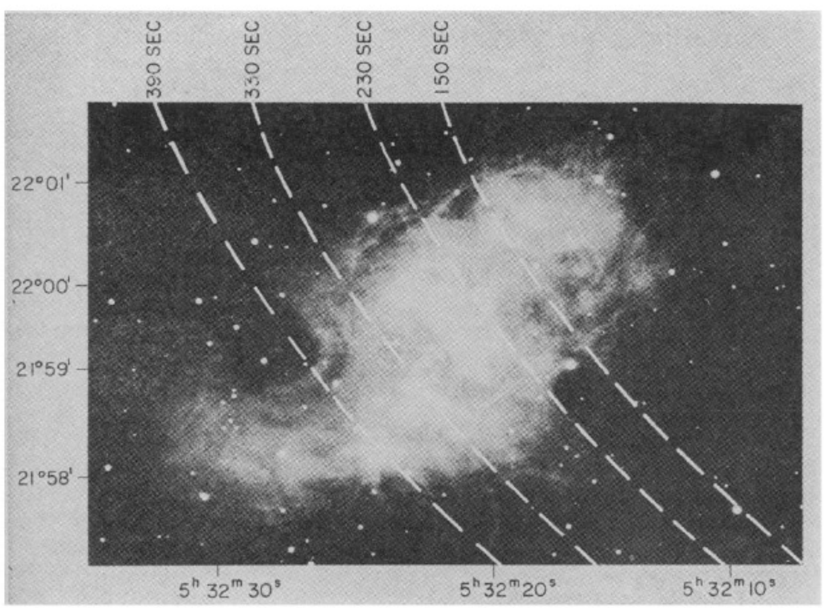

Figure 60s.4.3.2 - Progress of the occultation of the Crab Nebula measured in seconds of time after launch of the rocket from White Sands missile range. The dashed curves represent the position of the edge of the moon. A maximum rate of decrease in x-ray flux was observed at about 230 seconds (credit: NRL).

The occultation fixed the size scale of the X-ray Nebula but did not end the search for the pulsar. Subsequent events were driven by the discovery of radio pulsars, then of the radio pulses from the Crab in particular, which established the spin period. Next the optical object at the radio position, a star near the center of the nebula, was found pulsing with the same period. This situation meant that it was essential to search for the pulsar in the X-rays. An NRL sounding rocket was launched in 1969 (Mission: NB 3.210, Fritz et al. 1969) and found the X-ray pulses. This observation was the first detection of X-ray pulses from any source. By the date of the flight more sources like Sco X-1 had been found by NRL and other groups, and this result was the first rigorous demonstration of the neutron star nature of any of those point sources.

It was noted earlier that an additional decade was needed to accumulate sufficient evidence to prove that Sco X-1 was also a neutron star source, accreting from its companion in a binary system. Throughout that decade discovery and characterization of sources continued with many important developments, gradually revealing that the brightest X-ray sources in the Galaxy were neutron stars and black holes in binaries, made luminous by the accretion of matter onto the deep gravitational wells of expired stars. Most of these sources were highly luminous and many were surprisingly variable, and with launch of the *Uhuru* satellite the full diversity of the variability began to be seen. The surrounding context for the Dyson (1986) remark quoted above provides an apt summary that captures both the enduring intellectual impact in full breadth and the romance of the moment:

"… The relative values of different types of scientific information are a matter of personal taste. For me, however, the beginning of X-ray astronomy, which opened up a new window into the universe and revealed the existence of several new classes of astronomical objects, has been the most important single scientific fruit of the whole space program up till now. The newly discovered X-ray sources gave an entirely fresh picture of the universe, dominated by violent events, explosions, shocks, rapidly varying dynamical processes. The X-ray observations finally demolished the ancient Aristotelian view of the celestial sphere as a serene region populated by perfect objects moving in eternal peace and quietness. The old quiescent universe of Aristotle, which had survived essentially intact the intellectual revolutions associated with the names of Copernicus, Newton, and Einstein disappeared forever as soon as the X-ray telescopes went to work. And that new universe of collapsed objects and cataclysmic violence originated in the cheap little sounding rocket of the 1960s, popping up out of the Earth's atmosphere and observing the X-ray sky for only a few minutes before it fell back down."

4.0 The Discovery of X-rays from Cluster of Galaxies

Shortly after Edwin Hubble showed that galaxies existed independent of our own (1920s), it was recognized that most are members of groups or large clusters, the latter being the largest gravitationally bound structures as well as fundamental building blocks of the universe. By the late 1960s thousands of clusters had been cataloged from optical surveys. Calculation suggested that X-ray emission from normal galaxies within the clusters would be undetectable with the instruments available and sounding rocket observation times. However, Division rocket missions (see table and its references) would soon claim the discovery of X-ray emission from the most prominent of the nearby clusters: Virgo (to which our own galaxy within its Local Group belongs, Fig. 60s.4.4.1), Coma, and Perseus (Figs. 60s.4.4.2 and 60s.4.4.3).

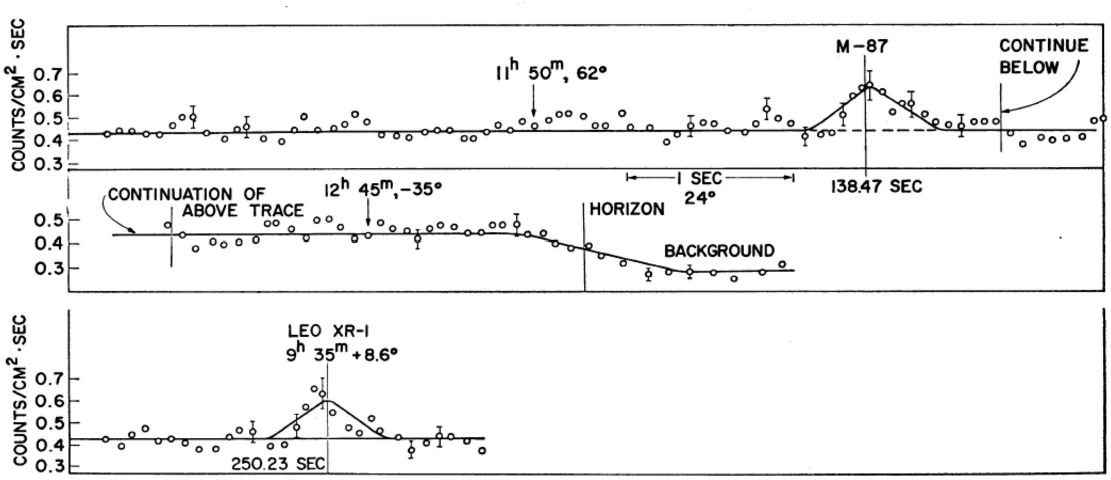

Fig. 9. Scans through M-87 and Leo XR-1.

Figure 60s.4.4.1 - Mission Apr 1965 (Byram et al. 1966): Discovery of X-ray emission from M-87 (Virgo cluster) (credit: NRL).

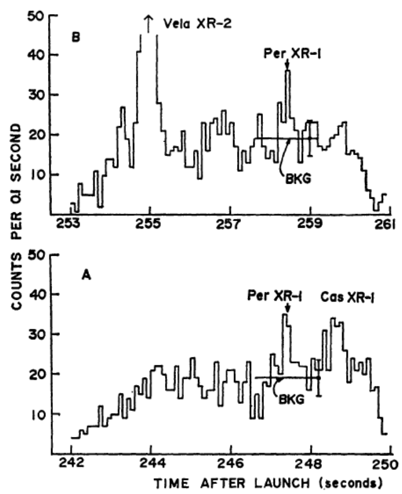

Figure 60s.4.4.2 - Mission NB 3.237 (Fritz et al. 1971): Discovery of X-ray emission from the Perseus cluster. X-ray Sources Cas XR-1 and Vel XR-2 are also detected. The low counting rates at the beginning and end of each scan is where the detectors are pointed below the horizon (credit: NRL).

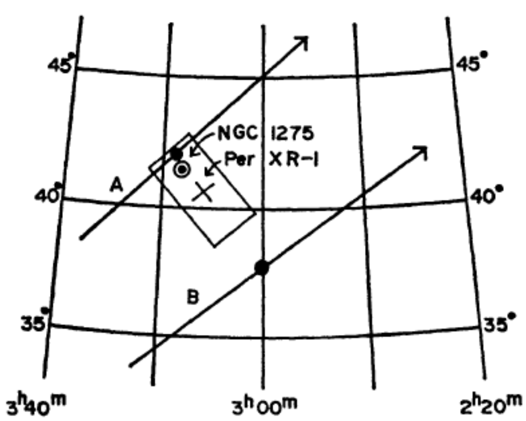

Figure 60s.4.4.3 - Mission NB 3.237 (Fritz et al. 1971): Most probable celestial location of Per X-1. The arrows show the path of the center of the field of view. Filled circles: position of peak counting rate; Cross, calculated position of the source. The area of the rectangle indicates the uncertainty in position measurement. The position of NGC 1275 is also indicated (credit: NRL).

In retrospect, X-ray emission from the Virgo and Perseus clusters *by itself* was arguably not a great surprise as both have prominent central galaxies. M87 in the Virgo cluster is a radio galaxy with synchrotron emission from its polarized optically-blue jet likely accounting for X-ray emission via the inverse-Compton mechanism. NGC 1275 in Perseus was already known as a Seyfert galaxy with strong radio and infrared emission and was therefore suspected to be a source of inverse-Compton X-ray emission (Fig. 60s.4.4.4). In effect both galaxies were prototypical examples of a source class that would eventually be known as "active galactic nuclei (AGN)", where X-ray emission is powered by material accreting onto a super massive black hole (~10^6 $M_\odot$) residing within the dominant galaxy at the center of the cluster's gravitational well. (Quasars are another type of AGN. X-ray emission from the nearest example, 3C273, was also discovered in a Division rocket mission, May 1967.) However, clusters like Coma without dominant galaxies were also found to be X-ray sources, thus leading to the surprising discovery of a hot (10^{6-7} K) thin intracluster gas emitting X-rays by the thermal bremsstrahlung mechanism in most if not all clusters. To even greater surprise was the result that the mass of hot intracluster gas was greater than that of its galaxies, making it the dominant baryon component in the universe. Moreover, this diffuse emission in clusters could account for a sizable fraction of the diffuse extragalactic X-ray background.

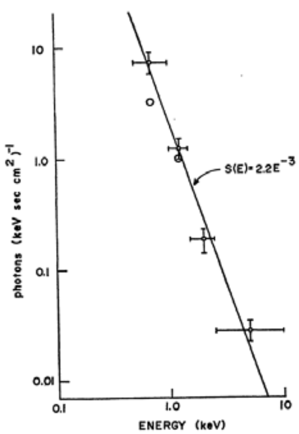

Figure 60s.4.4.4 - Mission NB 3.237 (Fritz et al. 1971): Spectrum of Per XR-1. The points plotted with error bars (± 1 σ, representing counting statistics only) have been corrected for ISM absorption, on the assumption the source is extragalactic. Open cirles: the low-energy spectrum uncorrected for absorption. A power-law spectrum fitting the data is shown. Note that the data binning and statistics do not allow a determination of whether an Fe-line feature exists at ~6 keV (credit: NRL).

5.0 Further 1970s-1980s Developments: Imaging & Orbital (Apollo-Soyuz, *SPARTAN-1*)

Orbital instruments were the most straightforward way to satisfy the urgent need for orders-of-magnitude increase in observation time and hence sensitivity. The first X-ray satellite, *Uhuru*, was launched in 1970 and completed a survey that significantly increased the number of known X-ray sources. The SSD response was the much larger and more capable *HEAO-1* A-1 experiment, described elsewhere in this history. However, it could not be ready for flight until 1977, and thus the SSD flew an interim rocket CPC on the 1975 Apollo-Soyuz mission. While this detector experienced a high background the useful science obtained included an accurate measurement of pulsations from the low-mass X-ray binary Small Magellanic Cloud SMC X-1, the discovery of X-ray emission from supernova remnant MSH 14-63 (Mills, Slee, & Hill),[11] and an upper limit to soft X-ray emission from the white dwarf HZ 43, which was however detected by an EUV instrument on this same mission. Ironically, HZ 43 is a benchmark white dwarf in understanding these endpoints of stellar evolution, a field the SSD would later enter (next section).

Just as urgent was the need for higher angular resolution to separate truly diffuse cluster emission from point-like AGN emission, and the SSD pursued two solutions. The technology to produce grazing incidence X-ray telescope mirrors and detectors with high spatial resolution was being developed rapidly by several groups. On missions 27.035 and 27.009 the SSD collaborated with the Max-Planck-Institut für Extraterrestrische Physik to fly such a telescope using *Röntgensatellit* (*ROSAT*) prototype mirrors. The detector for 27.035 was one of the first microchannel plate devices and was developed within the SSD. The detector for 27.009 was a prototype for the *ROSAT* position sensitive proportional counter. Both missions were technical successes and the experience gained formed part of the basis for the highly successful *ROSAT* and *J-PEX* (Joint Plasmadynamic astrophysics EXperiment) missions.

The SSD also pioneered the use of long (several degrees) but narrow (few arcmin) collimators on CPCs to achieve high resolution in one spatial dimension without sacrificing sensitivity (missions 26.047 to 26.053) and thus resolve point sources from crowded regions and/or those with diffuse emission. The apex of this effort was the *Spartan-1* mission (1985). *Spartan* (Shuttle Pointed Autonomous Research Tool for AstroNomy), co-developed by Cruddace, Fritz, and Shulman at NRL and the NASA Special Projects Division at GSFC, was a novel and successful concept that combined a payload derived from sounding rocket modular technology with Shuttle launch & recovery to produce a low-cost orbital mission (Fig. 60s.4.5.1).[12-13] The CPC X-ray detectors (Fig. 60s.4.5.2) used the long and narrow collimators[14] and data from multiple scans spanning 360º in position angle were used to produce tomographic maps of X-ray emission from the complex regions of the Galactic center and the Perseus cluster (Fig. 60s.4.5.3). These maps were effectively images of moderate resolution, complementary to those produced by the *Einstein* satellite's X-ray telescope, but with proportional counter spectral resolution and a much larger field of view. Analyses of the Perseus maps using a three-dimensional model produced two major results. First, the morphology and mass distributions were quantified out to a then-unprecedented radius of 1.6 Mpc. Second a radial gradient was discovered in the distribution of Fe as determined from 6-keV line (Fig. 60s.4.5.4). The new (1982) SSD Superintendent Herb Gursky viewed *Spartan-1* as a pathfinder that brought the decades-long SSD X-ray astrophysics sounding rocket program to a successful conclusion before what was to be a complete transition to Shuttle-deployed orbital instruments. However, the *Challenger* disaster (1986) completely reversed this plan.

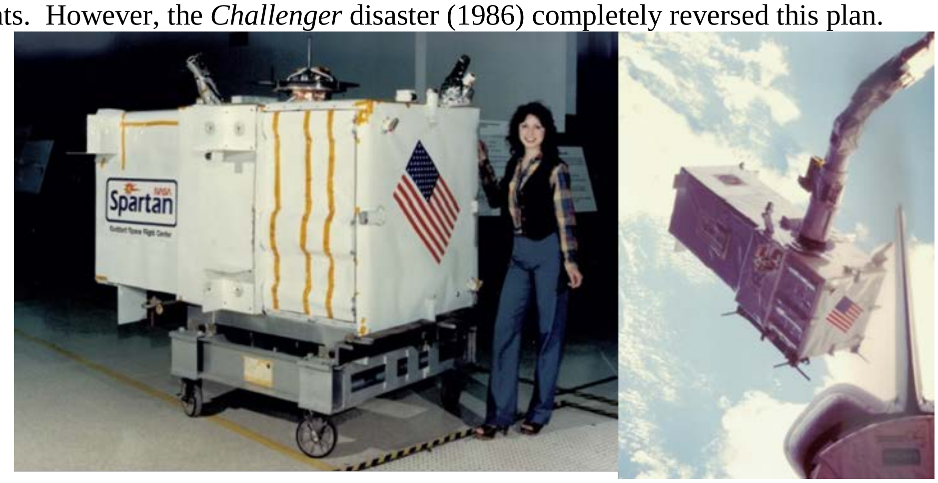

Figure 60s.4.5.1 - Spartan 1 payload: (left) after testing at NASA Kennedy Space Center, and (right) at retrieval by the Space Shuttle Discovery remote arm after deployment and operation (1985) (credit: NASA).

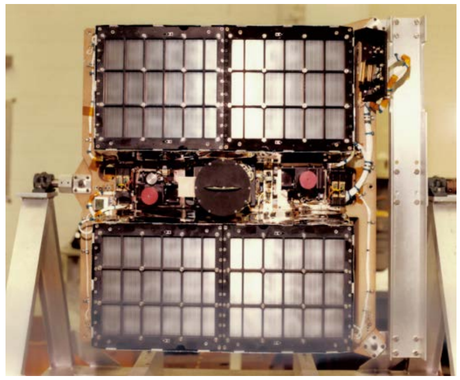

Figure 60s.4.5.2 - Spartan 1 X-ray instrument front, showing the four fine collimators (two per proportional counter), electronics, and two film-transport cameras (red covers) for calibration of the aspect solution (pointing direction). The bulk of the proportional counters lie behind the collimators (credit: NRL).

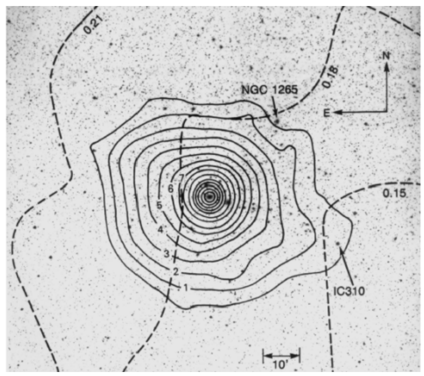

Figure 60s.4.5.3 - Smoothed map of the Perseus cluster diffuse X-ray emission (1-10 keV) derived from Spartan 1 scan data using a maximum entropy algorithm. Each of the 15 contours represents a factor of 1.5 change in X-ray surface brightness measured in units of counts cm-2 s-1 arcmin-2. The contours are superimposed on an optical photograph of the galaxies. The active galaxy NGC 1275 is at the cluster center of the emission, and a line of galaxies extends to the right ending at IC 310. The innermost contour represents a flux two-thirds of the peak values. The peak value is $2.5x10^{-3}$ counts cm^{-2} s^{-1} $arcmin^{-2}$, where $1x10^{-3}$ counts cm^{-2} s^{-1} $arcmin^{-2}$ equals $7x10^{-9}$ ergs cm^{-2} s^{-1} $arcmin^{-2}$. The X-ray emission is slightly elliptical and its centroid shifts to the right with increasing radius, indicating the cluster is not completely in equilibrium. The dashed line are contours of reddening, E(B-V), whose value is indicated on each contour, where 0.18 corresponds to N_H=$2.2x10^{21}$ cm^{-2}(credit: NRL).

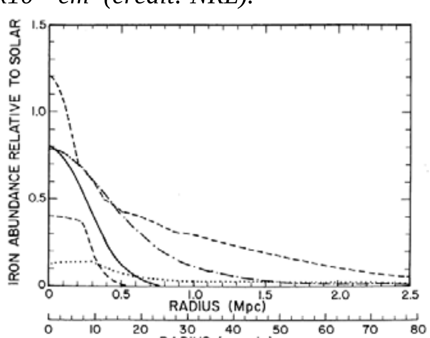

Figure 60s.4.5.4 - Best-fit (solid line) and envelope (dashed lines) of allowed Fe-abundance distributions for Gaussian model as derived from the Spartan 1 data. The dotted line was calculated for a theoretical model with an assumed gas mass-loss rate per galaxy of 10^{-11} yr^{-1} and the dot-dashed line was calculated for a model in which the galaxy mass-loss rate was proportional to the gas density (credit: NRL).

6.0 High-Resolution EUV Spectroscopy with *J-PEX*

Opportunities for Shuttle science missions were greatly reduced, thus phasing out the *Spartan* program and forcing a return to sounding rockets to maintain frequent access to space. However, the long exposures and high sensitivity provided by large orbital X-ray observatories (e.g., *ROSAT*, *Chandra*, *XMM*, *XTE*) now made rockets mostly non-competitive in the traditional X-ray (~0.1-10 keV) waveband. Fortunately, the opening of a new observational window (waveband) combined with a new technology again created exciting opportunities for astrophysics rocket missions.

The EUV had long been recognized as a critical waveband (~100-1000 Å / 100-10 eV) in understanding the physics of the solar corona and its effects on the Earth's ionosphere. This spectral region contains a wealth of plasma diagnostic edges and lines, mostly L-shell and thus complementary to the K-shell X-ray transitions, which span a broad range in temperature (~10^5-10^7 K) from all cosmologically important elements. Although the interstellar medium (ISM) strongly absorbs EUV radiation, Ray Cruddace demonstrated, using rocket data from several groups, that the local ISM density was lower than expected and its structure was patchy. This allowed astrophysics measurements over the waveband ~100-300 Å out to ~200 pc, the local region of our galaxy.[15] The *ROSAT* WFC and *EUVE* satellite missions compiled catalogs in the 1990s totaling over a thousand EUV sources, mostly stellar coronae, white dwarfs, and cataclysmic variables, but even some supernovae remnants and AGNs. However, the limited capability (~1 cm^2, $R=\lambda/\Delta\lambda$ ~200) of the *EUVE* spectrometer only hinted at what astrophysics might be produced if only sufficient effective area and *R* could be achieved, the former being limited primarily by the poor EUV (normal-incidence) reflectance of single-layer coatings of most materials.

The then-fledgling technology of multilayer coatings appeared promising, and so in 1990 SSD initiated research in this area, a collaborative effort between Cruddace and Kowalski in the X-ray Astronomy Branch (7620) and Seely in the Solar-Terrestrial Relationships Branch (7670). High-resolution EUV telescopes, microscopes, and above-all spectrometers used these coatings for space-based astronomical and solar work as well as for ground-based plasma research. Strong collaborations that endure today were developed with Troy Barbee, Jr., Lawrence Livermore National Laboratory, a pioneer in multilayer technology and with vendors of high quality mirrors and gratings (e.g., Carl Zeiss). It also took advantage of the NRL X24C beamline (Fig 60s.4.6.1), located at the National Synchrotron Light Source, Brookhaven National Laboratory, where all reflectance and efficiency calibrations were performed. Over two decades of work has now produced two major results. First, high values of multilayer reflectance are routinely achieved and these values are at or near theoretical limits. Modeling codes accurately predict performance and guide repeatable fabrication of stable multilayers. Second, an amazing result is that multilayer-coated gratings work as anticipated, where the multilayer enhances grating efficiency in the waveband and order of interest without degrading resolving power. Holographic ion-etched gratings were found to produce the highest efficiency because of their smooth surfaces and accurate groove profile (Fig. 60s.4.6.2), and these efficiencies are also near theoretical limits.

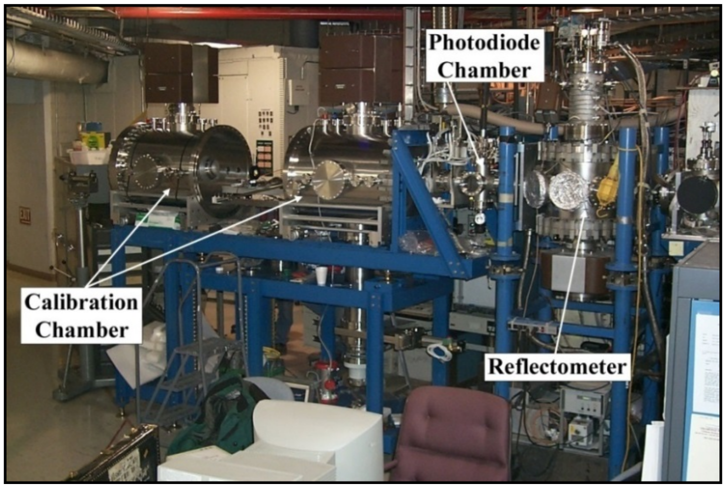

Figure 60s.4.6.1 - Beamline X-24C at the National Synchrotron Light Source, Brookhaven National Facility. This facility was used to develop multilayer-coated optics and is also capable of calibrating space-flight optics in the Reflectometer and the Calibration Chamber (credit: NRL).

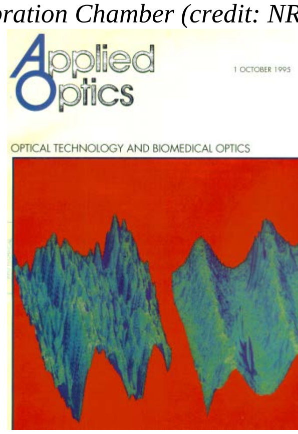

Figure 60s.4.6.2 - Cover issue of Applied Optics journal, showing our comparison of the surface of two blazed gratings, (left) fabricated by ruled-replication, and (right) fabricated by holographic ion-etching. It is evident that the latter technique produces smoother and more accurate grooves. The surfaces were characterized using an atomic force microscope (credit: NRL).

Solar EUV applications using multilayer technology are presented in the laboratory spectroscopy and *Hinode* essays elsewhere in this history. Success in astrophysics is represented by the *J-PEX* spectrometer. With its multilayer gratings (Fig. 60s.4.6.3) and microchannel plate detector together producing an instrument effective area ~7.5 cm^2 and *R*~4000, *J-PEX* is a pathfinder for EUV astrophysics.

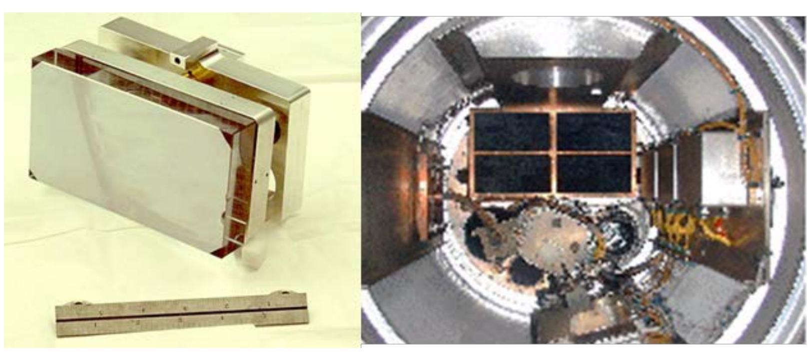

Figure 60s.4.6.3 (left) One of four J-PEX multilayer-coated gratings. (right) J-PEX aperture (credit: NRL).

J-PEX has so far made two successful rocket flights, where the scientific motivation was provided by collaboration with Martin Barstow, University of Leicester. The first (2001) produced the first high-resolution EUV spectrum for a non-solar object, the isolated white dwarf G191-B2B, and in the second flight (2008) the binary white dwarf Feige 24 was observed. The goals, which required high-resolution, were to detect photospheric Helium, leading to constraints on evolution models, to measure the amount of ionized Helium in the ISM along the line of sight, and to search for lines of heavier elements in the spectrum. The He II abundance measurements are possible *only* at EUV wavelengths where the Lyman series is present. The rich spectrum for G191-B2B (Fig. 60s.4.6.4) shows both ISM He II and metal lines. However, the results were also surprising because neither white dwarf produced a significant detection of a He II photospheric line, although model fits implied He was present. Expectations for photospheric He II detection were higher for Feige 24 because this white dwarf is a member of a binary system where Common Envelope evolution should have more likely stripped the mass of overlying Hydrogen. Formally, sensitive upper limits to the overlying layer of Hydrogen were obtained for both stars. Additionally, a high ionization fraction (He II/(He I + He II)) was derived in both cases that could be reconciled with measurements at other wavelengths only if a circumstellar component was included in the model fit at a level consistent with the *Hubble* Space Telescope Imaging Spectrograph (STIS) measurements. Finally, in contrast to previous results at other wavelengths, both studies showed that homogeneous models produced better fits than stratified ones. Clearly these objects are more complex than previously thought and more white dwarf observations are urgently needed.

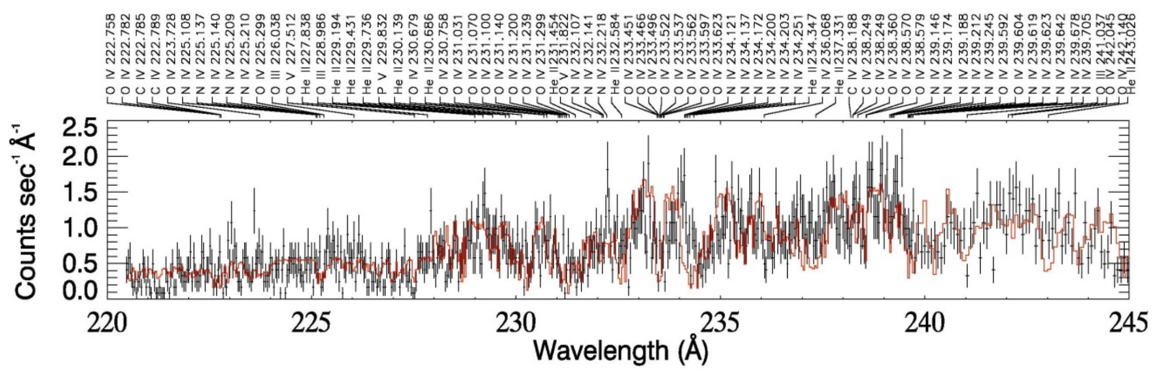

Figure 60s.4.6.4 - High-resolution EUV spectrum of G191-B2B obtained with J-PEX. All data points (black) have 1-σ error bars. The re histogram is the best-fit model of the star and the ISM. The strongest predicted lines of He, C, N, O, and P are labeled with their ionization state and wavelength. Lines of Fe and Ni, too numerous to include here, account for some unlabelled features and broader absorption structures (credit: NRL).

References: 60s.4: Rocket Astrophysics: 1960's, 1970's, and Beyond

1. "Upper Atmosphere Research Report No.XXXII, History of the Upper-Air Rocket-Research Program at the Naval Research Laboratory 1946-1957," Townsend, Jr., J.W., Friedman, H., and Tousey, R. 1958, NRL Report 5087, (Washington, DC: Naval Research Laboratory).
2. Friedman, H. "The Astronomer's Universe", (New York: W.W. Norton & Co., Inc., 1990), pg 129
3. "Experiment research US progr. for IGY to 1.7.58," Kupperian, Jr., J.E., and Friedman, H. 1958, IGY Rocket Report Ser. (1): 201
4. "Intensity of the Soft X-ray Background Flux: Reply to Bowyer and Field," Henry, R.C., Fritz, G., Meekins, J.F., Friedman, H., and Byram, E.T. 1970, Nature, **225**, 5230
5. "Line Emission in the X-ray Background," Shulman, S., Fritz, G., Meekins, J.F., Chubb, T.A., and Friedman, H. 1971, ApJ, **166**, L9

6. “The Soft X-ray Background,” Friedman, H., Fritz, G., Shulman, S.D., and Henry, R.C. 1973, X- and Gamma-Ray Astronomy,” COSPAR Symposium, eds., H. Brandt and R. Giacconi, 215
7. "Evidence for X-rays from sources outside the solar system," Giacconi, R. Gursky, H. Paolini, F.R. Rossi, B.B., 1962, Phys. Rev. Lett. **9**, 439
8. “The Identification of the Coronal Lines,” Edlén, B. 1945, M.N.R.A.S., **105**, 323E (George Darwin Lecture)
9. “Reminiscences of 30 Years of Space Research,” Friedman, H. 1977, NRL Report 8113, (Washington, DC: Naval Research Laboratory).
10. Harwit, M. “Cosmic Discovery: The Search, Scope, and Heritage of Astronomy,” (New York: Basic Books, Inc., 1981), pg 15
11. “A catalogue of radio sources between declinations +10 and -20,” Mills, B.Y., Slee O.B., Hill, E.R. 1958, Australian J. Phys., **11**, 360-387
12. “SPEAR: Small Payload Ejection and Recovery for the Space Shuttle,” Cruddace, R.G., Fritz, G.G., and Shulman, S. 1977, Astronautics & Aeronautics, Jan 1977, 42
13. “The SPARTAN 1 Mission,” Cruddace, R.G., Brandenstein, D.C., Creighton, J.O., Fabian, J.M., Fenimore, E.E., Fritz, G.G., Gross, C., Gutschewski, G., Lucid, S.W. Nagel, S.R., Shrewsberry, D.J., and Zimmerman, D. 1990, Journal of The British Interplanetary Society, **43**, 223
14. “The SPARTAN 1 Collimated X-ray Detector System,” Fritz, G.G., Cruddace, R.G., Kowalski, M.P., Snyder, W.A., Tait, R.M., Woods, D.W., Fenimore, E.E., Serna, E., Middleditch, J. and Ulmer, M.P. 1995, NRL Memorandum Report 7620-95-7737
15. “On the Opacity of the Interstellar Medium to Ultrasoft X-rays and Extreme-Ultraviolet Radiation,” Cruddace, R., Paresce, F., Bowyer, S., and Lampton, M. 1974, ApJ, **187**, 497

Table References: 60’s.4 Rocket Astrophysics: 1960’s, 1970’s, and Beyond

Mission: Apr 1963
“X-ray Emission from the Direction of Scorpius,” Bowyer, S., Byram, E.T., Chubb, T.A., and Friedman, H. 1964, AJ, **69**, 135
“X-ray Sources in the Galaxy,”, Bowyer, S., Byram, E.T., Chubb, T.A., and Friedman, H. 1964, Nature, **201**, 1307

Mission: Jun 1964, Nov 1964
“Cosmic X-ray Sources,” Bowyer, S., Byram, E.T., Chubb, T.A., and Friedman, H. 1965, Science, **147**, 394

Mission: Jul 1964
“Lunar Occultation of X-ray Emission from the Crab Nebula,” Bowyer, S., Byram, E.T., Chubb, T.A., and Friedman, H. 1964, Science, **146**, 912

Mission: Apr 1965
“Cosmic X-ray Sources, Galactic and Extragalactic,” Byram, E.T., Chubb, T.A., and Friedman, H. 1966, Science, **152**, 66
“Distribution and Variability of Cosmic X-ray Sources,” Friedman, H., Byram, E.T., and Chubb, T.A. 1967, Science, **156**, 3773

Mission: May 1967
“X-rays from Sources 3C 273 and M87,” Friedman, H. and Byram, E.T. 1967, Science, **158**, 257

Mission: NB 3.196
“New X-Ray Spectra of Sco XR-1, Cyg XR-1, and Cyg XR-2,” Meekins, J.F., Fritz, G., Henry, R.C., Byram, E.T., and Friedman, H. 1968, AJ, **73**, S106
“Possible Detection of a Dense Hot Intergalactic Medium,” Fritz, G., Meekins, J.F., Henry, R.C.,

Byram, E.T., and Friedman, H. 1968, AJ, **73**, S106

"Possible Detection of a Dense Hot Intergalactic Medium," Fritz, G., Meekins, J.F., Henry, R.C., Byram, E.T., and Friedman, H. 1968, ApJ, **153**, L11

"Soft X-rays from Scorpius XR-1", Fritz, G., Meekins, J.F., Henry, R.C., Byram, E.T., and Friedman, H. 1968, ApJ, **153**, L199

"On X-ray Line Emission from Scorpius XR-1", Fritz, G., Meekins, J.F., Henry, R.C., and Friedman, H. 1969, ApJ, **156**, L33

"X-ray Spectra of Several Discrete Cosmic Sources," Meekins, J.F., Henry, R.C., Fritz, G., Friedman, H., and Byram, E.T. 1969, ApJ, **157**, 197

"X-ray Intensity Fluctuations in Cygnus XR-1," Shulman, S., Fritz, G., Meekins, J.F., and Friedman, H. 1971, ApJ, **168**, L49

"Evidence for a Compact Source of Soft X-rays in the Cygnus Loop," Bleach, R.D., Henry, R.C., Meekins, J.F., Fritz, G., Shulman, S.D., and Friedman, H. 1975, ApJ, **197**, L13

<u>Mission: Apr 1968</u>

"X-ray Survey of Centaurus A," Byram, E.T., Chubb, T.A., and Friedman, H. 1970, Science, **169**, 366

<u>Mission: NB 3.210 / NASA 4.290</u>

"X-ray Pulsar in the Crab Nebula", Fritz, G., Henry, R.C., Meekins, J.F., Chubb, T.A., and Friedman, T.A. 1969, Science, **164**, 709

"Excess Background Radiation of Soft X-Rays at the Galactic Pole and Plane," Henry, R.C., Fritz, G., Meekins, J.,F., Chubb, T.A., and Friedman, H., 1971, ApJ, **163**, L73

"The X-ray Spectra of the Crab Nebula and NP 0532," Fritz, G., Meekins, J.F., Chubb, T.A., and Friedman, H. 1971, ApJ, **164**, L55

"X-Rays from the Coma Cluster of Galaxies," Meekins, J.F., Fritz, G., Chubb, T.A., and Friedman, H. 1971, Nature, **231**, 107

"Absorption of Crab Nebula X-rays," Henry, R.C., Fritz, G., Meekins, J.F., Chubb, T.A., and Friedman, H. 1972, ApJ, **174**, 389

<u>Mission: NB 3.237</u>

"Discovery of an X-ray Source in Perseus," Fritz, G., Davidsen, A., Meekins, J.F., and Friedman, H. 1971, ApJ, **164**, L81

"Observations of the Soft X-ray Background," Davidsen, A., Shulman, S., Fritz, G., Meekins, J.F., Henry, R.C., and Friedman, H. 1972, ApJ, **177**, 629

"Far-Ultraviolet Studies. II. Galactic-Latitude Dependence of the 1530 Å Interstellar Radiation Field," Henry, R.C., Swandic, J.R., Shulman, S., and Fritz, G. 1977, ApJ, **212**, 707

<u>Mission: NB 4.244</u>

"Soft X-rays from IC443," Shulman, S., Naranan, S., Fritz, G., and Friedman, H. 1976, Astrophysical Letter, **17**, 15

<u>Mission: NB 4.257</u>

"Soft X-ray Emission in Eridanus: An Old Supernova Remnant?" Naranan, S., Shulman, S., Friedman, H., and Fritz, G. 1976, ApJ, **208**, 718

<u>Mission: NASA 13.091</u>

"Soft X-ray Emission from Hercules X-1," Shulman, S., Friedman, H., Fritz, G., Henry, R.C. and Yentis, D.J. 1975, ApJ, **199**, L101

"X-ray Evidence for the Supernova Origin of the North Polar Spur," Cruddace, R.G., Friedman, H., Fritz, G., and Shulman, S. 1976, ApJ, **207**, 888

<u>Mission: NASA 13.100</u>

"Discovery of X-ray Pulsations in SMC X-1," Lucke, R., Yentis, D., Friedman, H., Fritz, G., and Shulman, S. 1976, ApJ, **206**, L25

Mission: NASA 26.025

"Soft X-rays from Hercules X-1 During the "Off" State," Fritz, G., Naranan, S., Shulman, S., Yentis, D., and Friedman, H. 1976, ApJ, **207**, L29

"Soft X-ray Sources and Supernova Remnants in Cygnus: Rocket and Apollo-Soyuz Results," Davidsen, A.F., Henry, R.C., Snyder, W.A., Friedman, H., Fritz, G., Naranan, S., Shulman, S., and Yentis, D. 1977, ApJ, **215**, 541

"Soft-X-ray Emission from a Newly Discovered Supernova Remnant in Cygnus," Snyder, W.A., Davidsen, A.F., Henry, R.C., Shulman, S., Fritz, G., and Friedman, H. 1978, **222**, L13

Mission: Apollo-Soyuz

"Soft X-ray Observations," Shulman, S., Naranan, S., Snyder, W., Yentis, D., Cruddace, R., Friedman, H., Fritz, G., and Henry, R. 1977, ASTP Summary Science Report, NASA SP-412, **I**, 39

"X-ray Emission from the Supernova Remnant MSH 14-63," Naranan, S., Shulman, S., Yentis, D., Fritz, G., and Friedman, H. 1977, ApJ, **213**, L53

Mission: NASA 26.049

"High-Resolution Observations of X-ray Sources at the Galactic Center," Cruddace, R.G., Fritz, G., Shulman, S., and Friedman, H. 1978, ApJ, **222**, L95

Mission: NASA 26.052 & 26.053

"Observations of the Structure of the Diffuse X-ray Emission from the Coma Cluster," Johnson, M.W., Cruddace, R.G., Fritz, G., Shulman, S., and Friedman, H. 1979, **231**, L45

"Soft X-ray Sources in the Bar of the Large Magellanic Cloud," McKee, J.D., Fritz, G., Cruddace, R.G., Shulman, S., and Friedman, H. 1980, ApJ, **238**, 93

Mission: SPARTAN-1

"SPARTAN-1 X-ray Observations of the Perseus Cluster: Comparison of the Iron Abundances and Temperatures in the Inner and Outer Regions of the Cluster," Ulmer, M.P., Cruddace, R.G., Fenimore, E.E., Fritz, G.G., Snyder, W.A. 1987, ApJ, **319**, 118

"X-ray Observations of the Galactic Center by SPARTAN 1," Kawai, N. Fenimore, E.E., Middleditch, J., Cruddace, R.G., Fritz, G.G., Snyder, W.A., and Ulmer, M.P. 1988, ApJ, **330**, 130

"SPARTAN 1 X-ray Observations of the Perseus Cluster. II. The Distribution of Flux and Hardness Ratio out to a Radius of 50 Arcminutes," Snyder, W.A., Kowalski, M.P, Cruddace, R.G., Fritz, G.G., Middleditch, J., Fenimore, E.E., Ulmer, M.P. and Majewski, S.R. 1990, ApJ, **365**, 460

"SPARTAN 1 X-ray Observations of the Perseus Cluster. III. The Distribution of Iron in the Intracluster Gas," Kowalski, M.P., Cruddace, R.G., Snyder, W.A., Fritz, G.G., Ulmer, M.P., and Fenimore, E.E. 1993, ApJ, **412**, 489

"The Baryon Fraction in the Perseus Cluster: Results from SPARTAN 1," Cruddace, R.G., Kowalski, M.P., Fritz, G.G., Snyder, W.A., Fenimore, E.E., and Ulmer, M.P. 1997, ApJ, **476**, 479

Mission: NASA 36.195

"High-Resolution Spectroscopy of G191-B2B in the Extreme Ultraviolet," Cruddace, R.G., Kowalski, M.P. Yentis, D., Brown, C.M., Gursky, H., Barstow, M.A., Bannister, N.P., Fraser, G.W., Spragg, J.E., Lapington, J.S., Tandy, J.A., Sanderson, B., Culhane, J.L., Barbee, T.W., Kordas, J.F., Goldstein,W., and Fritz, G.G., 2002, ApJ,. **565**, L47

"High-Resolution Extreme Ultraviolet Spectroscopy of G191-B2B: structure of the stellar photosphere and the surrounding interstellar medium," Barstow, M.A., Cruddace, R.G., Kowalski, M.P., Bannister, N.P., Yentis, D., Lapington, J.S., Tandy, J.A., Hubeny, I., Schuh, S., Dreizler, S., and Barbee, T.W. 2005, M.N.R.A.S., **362**, 1273

Mission: NASA 36.207

"High-Resolution Spectroscopy of Feige 24 in the Extreme-Ultraviolet," Kowalski, M.P., Barstow, M.A., Wood, K.S., Yentis, D.J., Fritz, G.G., Lapington, J.S., Barbee, Jr., T.W., Berendse, F.B., and Cruddace, R.G. 2011, ApJ, **730**, 115

A1. **List of Terms and Acronyms**

Preface
- SSD – Space Science Division
- NRL – Naval Research Laboratory

60s Decade
- OGO - Orbiting Geophysical Observatory
- OSO - Orbiting Solar Observatory
- STP – Space Test Program
- UV – Ultraviolet
- EUV - Extreme Ultraviolet

60s.1
- SSULI – Special Sensor Ultraviolet Limb Imager
- DMSP – Defense Meteorological Satellite Program
- FUV - Far Ultraviolet
- OGO - Orbiting Geophysical Observatory
- OSO – Orbiting Solar Observatory
- DOD – Department of Defense
- NASA/TIMED – National Aeronautics and Space Administration Thermosphere, Ionosphere, Mesosphere Energetics and Dynamics
- GUVI - Global Ultraviolet Imager
- RAIDS - Remote Atmospheric and Ionospheric Detection System
- EUV - extreme ultraviolet
- FOV – Field of View

60s.2
- UV – Ultraviolet
- SMM - Solar Maximum Mission
- GSFC – Goddard Space Flight Center
- CME(s) - Coronal Mass Ejection(s)
- SEC – Secondary Emission Cathode
- NOAA - National Oceanic and Atmospheric Administration

60s.3
- SOLRAD - Solar Radiation
- NSSDC - National Space Science Data Center
- GOES - Geostationary Orbiting Environmental Satellites
- SID - Sudden Ionospheric Disturbance

60s.4
- CPC Collimated Proportional Counter
- ISM - Intervening Interstellar Medium
- AS&E - American Science & Engineering's
- RXTE - Rossi X-ray Timing Explorer
- AGN - Active galactic nuclei
- SMC - Small Magellanic Cloud
- Spartan - Shuttle Pointed Autonomous Research Tool for AstroNomy
- ROSAT - Röntgensatellit
- J-PEX - Joint Plasmadynamic astrophysics EXperiment
- ISM - Interstellar medium
- STIS - Space Telescope Imaging Spectrograph